Dysregulation of the p53 pathway provides a therapeutic target in aggressive pediatric sarcomas with stem-like traits

Lucie Curylova[1,2], Iva Staniczkova Zambo[1,3], Jakub Neradil[1,2], Michal Kyr[1,4], Nicola Jurackova[1,3], Sarka Pavlova[5,6], Kristyna Polaskova[1,4], Peter Mudry[4], Jaroslav Sterba[4], Renata Veselska[1,2], Jan Skoda[1,2,*]

[1]Department of Experimental Biology, Faculty of Science, Masaryk University, 625 00 Brno, Czech Republic

[2]International Clinical Research Center, St. Anne's University Hospital, 656 91 Brno, Czech Republic

[3]1st Department of Pathology, St. Anne's University Hospital and Faculty of Medicine, Masaryk University, Brno, Czech Republic

[4]Department of Pediatric Oncology, University Hospital Brno and Faculty of Medicine, Masaryk University, 613 00 Brno, Czech Republic

[5]Central European Institute of Technology (CEITEC), Masaryk University, 625 00 Brno, Czech Republic

[6]Department of Internal Medicine, Hematology and Oncology, University Hospital Brno and Faculty of Medicine, Masaryk University, 625 00 Brno, Czech Republic

*__Corresponding Author:__
Dr. Jan Skoda (ORCID 0000-0002-9292-8177)
Department of Experimental Biology, Faculty of Science, Masaryk University
University Campus Bohunice - C13.326
Kamenice 5
625 00 Brno, Czech Republic
Phone: +420 549 49 8021; Email: jan.skoda@sci.muni.cz

Competing interests: The authors declare no competing financial interests.

Word count (Main body of text): 3476
Figures: 6 Suppl. Fig: 14 Suppl. Tables: 4 Ref: 48

HIGHLIGHTS

- SOX2 and KLF4 factors are crucially involved in pediatric sarcoma development
- Dysregulated p53 pathway predisposes sarcoma cells to a fully stem-like phenotype
- p53 positivity associates with early metastasis in pediatric sarcoma patients
- Restoring wild-type p53 activity selectively targets stem-like Ewing's sarcomas

ABSTRACT

Pediatric sarcomas are bone and soft tissue tumors that often show high metastatic potential and refractory stem-like phenotypes with poor outcomes. Aggressive sarcomas frequently harbor disrupted p53 pathway. However, whether the abrogated p53 function associates with sarcoma stemness which might be targeted by p53 reactivation remains unclear. Here we show that aggressive stem-like sarcoma cells exhibit deregulated p53, making them vulnerable to drugs that restore the wild-type p53 activity. Immunohistochemistry in mice xenografts and human tumor tissues revealed that p53 deregulations together with the enhanced expression of SOX2 or KLF4 stemness-related transcription factors are crucial in the development of pediatric osteosarcoma, rhabdomyosarcoma, and Ewing's sarcoma. Alteration of p53 function appears to be an important step for attaining a fully stem-like phenotype in sarcoma cells and p53-positive pediatric sarcomas show high frequency of early metastasis. Moreover, the reactivation of p53 via MDM2/MDMX inhibition selectively induces cell death in aggressive stem-like Ewing's sarcoma cells, while sparing healthy fibroblasts. Collectively, our results demonstrate that restoration of p53 canonical activity may represent a promising strategy for improving therapy of pediatric sarcomas with unfavorable stem-like traits.

KEYWORDS

pediatric sarcomas; cancer stemness; p53; prognosis; targeted therapy

ABBREVIATIONS

ES	Ewing's sarcoma
FFPE	formalin-fixed paraffin-embedded
IHC	immunohistochemistry
mut-p53	mutant p53
NGS	next-generation sequencing
OS	osteosarcoma
RMS	rhabdomyosarcoma
shCtrl	shRNA control
shSOX2	shRNA-mediated knockdown of SOX2
SI	stemness index
TF	transcription factor
TMA	tissue microarray
wt-p53	wild-type p53

1. INTRODUCTION

Sarcomas are common pediatric tumors, accounting for up to 15% of all malignancies diagnosed in children. These soft tissue and bone tumors most likely originate from deregulated mesenchymal stem cells and their derivatives [1,2]. Despite intensive multimodal therapy, about one-third of pediatric sarcoma patients experience disease recurrence, therapy resistance and metastasis–traits commonly linked to cancer stemness–which subsequently results in a dismal survival of only 20% [3,4]. Understanding the mechanisms that underlie the development of these aggressive therapy-resistant tumors is therefore crucial for improving management and therapy of pediatric sarcomas.

Besides several putative markers [3,5–7], expression of key pluripotency-related transcription factors (TFs), i.e., SOX2, OCT4, NANOG, KLF4 and c-MYC [8], has been linked to the stem-like phenotype of sarcoma cells [9–13]. Upregulation of these TFs is well known to alter cell proliferation, differentiation and plasticity [8,14], highlighting them as core functional regulators of the stem-like state and potential mediators of sarcoma tumorigenesis. Nevertheless, a question remains if the expression signatures of these TFs, considered either individually or in combination, might serve as determinants of pediatric sarcoma aggressiveness, predicting patient outcomes.

p53 was primarily recognized as a crucial tumor suppressor. Recently, it has been also identified as a regulator of stemness maintenance and differentiation in both healthy and tumor tissues [1,15]. Its activity was found to restrict cancer stem cell self-renewal and inhibit tumor initiation and progression [15]. Given that *TP53* mutations and other deregulations of the p53 pathway (*e.g.*, *MDM2* amplification) are frequently observed in majority of human sarcomas [1], targeting p53 might potentially provide a strategy to suppress sarcoma stemness. Several approaches to restore wild-type p53 (wt-p53) function have been designed to date, including gene therapy, direct reactivation or depletion of mutant p53 (mut-p53), and inhibition of p53 negative regulators from the MDM family (reviewed in [1]). However, whether p53 deregulation is related to the stemness of pediatric sarcomas has remained unknown.

This study aimed to elucidate the potential connection between the dysregulated stemness-related transcriptional network and p53 alterations in pediatric sarcomas. Furthermore, it investigated whether restoring normal p53 activity might effectively target aggressive, stem-like sarcoma cells. By

employing a unique panel of established and patient-derived osteosarcoma (OS), rhabdomyosarcoma (RMS) and Ewing's sarcoma (ES) cell lines, we provide strong evidence that links p53 deregulations together with the upregulated expression of selected stemness-related TFs and aggressive tumorigenic features of pediatric sarcoma cells. Interestingly, we identified dysregulated p53 pathway as the most consistent factor contributing to the development of stem-like, tumorigenic phenotype of sarcoma cells. Fully expressed stem cell characteristics were exclusively observed in models with altered p53. Consistently, immunohistochemistry analysis in a cohort of pediatric OS, RMS and ES confirmed that p53 positivity associates with metastatic potential. Expanding on our findings, this work provides first insights into the therapeutic potential of targeting sarcoma stemness via p53. Restoring the p53 activity proved to preferentially target aggressive stem-like ES cells compared with their nontumorigenic counterparts or healthy fibroblasts. Our findings indicate that reactivation of deregulated p53 pathway is a clinically relevant strategy to enhance the treatment of aggressive pediatric sarcomas.

2. MATERIALS AND METHODS

2.1. Cell culture and treatment

The following cell lines were used in this study: (i) a panel of in-house patient-derived OS (n=10), RMS (n=10) and ES (n=12) cell lines (listed in Supplementary Table 1) which were established from tumor tissues with written informed consent under previous projects (IGA MZCR NR9125-4, IGA MZCR NT13443-4, OP VVV CZ.02.1.01/0.0/0.0/16_019/0000868) and their use for this study was approved by the Masaryk University Research Ethics Committee, Brno, Czech Republic (approval no. EKV-2019-051); (ii) established sarcoma cell lines MNNG/HOS (OS, purchased from ECACC, #87070201), HuO-3N1 (OS, purchased from JCRB, #JCRB0413), SAOS-2 (OS, purchased from ATCC, #HTB-85) and RD (RMS, purchased from ECACC, #85111502); (iii) NTERA-2 (human pluripotent embryonal carcinoma cell line, clone D1) purchased from ECACC (#01071221) served as a positive control; (iv) NDF-2 and NDF-3 (human neonatal dermal fibroblast cell lines, #CC-2509; Lonza Bioscience, Durham, NC, USA; a kind gift of Dr. Tomáš Bárta). All cell lines were authenticated by STR profiling (Generi Biotech, Hradec Králové, Czech Republic) and routinely tested for mycoplasma by PCR. Culture media supplements are listed in Supplementary Table 2. All cell lines were cultured in a humidified 5% CO2 atmosphere at 37°C.

Drugs targeting p53 pathway were used for the treatment: RO-5963 (MDM2/MDMX dual inhibitor, #444153, Sigma-Aldrich, St. Louis, MO, USA) and PRIMA-1^{MET} (mut-p53 reactivator, #SML1789, Sigma-Aldrich). Drug treatments were performed following day after seeding.

2.2. Tumor samples

Formalin-fixed paraffin-embedded (FFPE) tumor tissue samples were obtained from 91 pediatric sarcoma patients (male/female: 54/37; age at diagnosis: 12 ± 5.6 years) treated at the University Hospital Brno or St. Anne's University Hospital between 2006 and 2020. The study cohort consisted of 34 OS, 22 RMS (14 alveolar RMS, 7 embryonal RMS) and 36 ES initial biopsies. In total, 38 OS, 31 RMS and 41 ES biopsies were analyzed in this study. All samples were obtained with written informed consent and their use for this study was approved by the Masaryk University Research Ethics Committee, Brno, Czech Republic (approval no. EKV-2019-051).

2.3. Western blotting

Western blotting and densitometry were performed as previously described [16]. Following antibodies were used for immunoblotting analysis: rabbit anti-SOX2 (1:1000; #3579, Cell Signaling Technology, CST, Danvers, MA, USA), rabbit anti-OCT4 (1:1000; #2750, CST), rabbit anti-NANOG (1:1000; #4903, CST), rabbit anti-c-MYC (1:1000; #5605, CST), rabbit anti-KLF4 (1:1000; #ab215036, Abcam, Cambridge, UK), mouse anti-p53 (1:10,000; #P6874, Sigma-Aldrich), mouse anti-MDM2 (1:500; #sc-965, Santa Cruz Biotechnology, SCBT, Dallas, Texas, USA), mouse anti-p63 (1:200, #sc-25268, SCBT) rabbit anti-p73 (1:1000, #sc-2750, SCBT), mouse anti-MDMX (1:200, #sc-74468, SCBT), rabbit anti-cleaved caspase-3 (1:1000; #9664, CST), rabbit anti-GAPDH (1:10,000, #2118, CST) and mouse anti-β-actin (1:10,000, #A5441, Sigma-Aldrich). GAPDH and β-actin served as loading controls.

2.4. Stemness index calculation

Relative values (to the loading control) of the protein expression of SOX2, OCT4, NANOG, KLF4 and c-MYC stemness-associated transcription factors were used to calculate stemness index for each sarcoma cell line. Stemness index of each cell line was determined as follows: sum of expression values of individual stemness factors after their division by the mean expression of the respective stemness factor in the given sarcoma subtype (OS, RMS, or ES).

2.5. RT-qPCR

RNA extraction, reverse transcription (with equal amounts of 20 ng of RNA per 1 µl of the reaction mix) and qPCR were performed as previously [16]. Primer sequences are listed in Supplementary Table 3. All qPCR reactions were performed in technical triplicates.

2.6. TP53 mutation analysis

In selected cell lines, amplicon ultra-deep next generation sequencing (NGS) of the whole coding region of *TP53* gene was performed and assessed as previously described [17].

2.7. shRNA-mediated SOX2 knockdown

shRNA lentiviral particles were utilized to knockdown expression of SOX2 (#sc-38408-V, SCBT). Experiments were performed as per manufacturer's instructions. Scrambled shRNA lentiviral particles (#sc-108080, SCBT) were used to establish respective controls. Single-cell clones were isolated from

both stable shRNA control and SOX2 knockdown cell pools using puromycin (#sc-108071, SCBT) as the selection agent.

2.8. MTT assay

Cells were seeded in 96-well plates in a density of 5000 and 2000 cells/well, respectively, for 72h treatment with selected drugs. Cell viability was measured after the exposure time using MTT assay by adding thiazolyl blue tetrazolium bromide (#M2128, Sigma-Aldrich) to reach the final concentration of 455 µg/ml. Medium was replaced with 200 µl of DMSO after 3h incubation under standard conditions followed by measurement of absorbance by Sunrise Absorbance Reader (Tecan, Männedorf, Switzerland). Half maximal inhibitory concentration (IC_{50}) of drugs was determined using non-linear regression of datasets of MTT assay calculated by GraphPad Prism 8.0.2. software (GraphPad Software, San Diego, CA, US), absolute IC_{50} value was determined by the following formula: relative IC50*(((50-top)/(bottom-50))^(−1/hill slope)).

2.9. Limiting dilution sphere formation assay

Cells were harvested and dissociated into single-cell suspension by accutase (Biosera, Cholet, France), re-suspended in a defined serum-free medium: DMEM Low Glucose (#LM-D1100, Biosera) based medium w/o FCS, supplemented with 10 ng/mL EGF (Sigma-Aldrich), 20 ng/mL FGF2 (Sigma-Aldrich), and 1× B-27 supplement w/o vitamin A (Gibco, Carlsbad, CA, USA); and serially diluted and cultured as described in [16]. Spheres were evaluated after one week and only spheres with ≥50 µm in diameter were analyzed using live cell imaging system Incucyte® SX1 (Sartorius, Göttingen, Germany). Frequencies of sphere-forming cells among experimental groups were calculated and compared using ELDA software [18].

2.10. Tumorigenicity assay *in vivo* and tissue microarray assembly

Cells were harvested, enzymatically dissociated and a single-cell suspension of 1×10^6 cells in 100 µl of based DMEM Low Glucose medium was injected subcutaneously into the right flank of nine-week-old NSG (NOD/ShiLtSz-*scid/I12rγ*^{null}) mice. All animal experiments were conducted in accordance with a study (MSMT-4408/2016-6) approved by the Institutional Animal Care and Use Committee of Masaryk University and registered by the Ministry of Education, Youth and Sports of the Czech Republic as required by national legislation. Experiments were terminated after reaching sufficient tumor volume (500 mm^3) or after 25 weeks. Xenograft tissues were embedded into FFPE

blocks and processed for tissue microarray (TMA) assembly. Briefly, tumor core biopsies (Ø3 mm) were punched from annotated donor blocks according to hematoxylin-eosin staining of the whole xenograft sections and re-embedded into a positionally encoded array of the recipient block casted manually using the Simport M473 T-Sue™ Microarray Mold Kit (#M473-36, Simport Scientific, Beloeil, Canada) as per manufacturer's instructions.

2.11.Flow cytometry

Cells were harvested after the exposure to the treatment and enzymatically dissociated in a single-cell suspension in PBS containing 3% fetal bovine serum (#FB-1101, Biosera) and 2mM EDTA (#ED2SS, Sigma-Aldrich). Measurement of cell viability was performed after 15-minute incubation with 5 nM SYTOX™ Red Dead Cell Stain (#S34859, Invitrogen, Carlsbad, CA, USA) on ice using CytoFLEX S flow cytometer (Beckman Coulter, Brea, CA, USA).

2.12.Immunohistochemistry

Immunohistochemistry (IHC) staining was performed using Ventana BenchMark ULTRA IHC/ISH System (Roche, Rotkreuz, Switzerland). For both sarcoma xenograft TMA and human sarcoma tissues, 1.5-micron-thick sections were deparaffinized by EZ Prep Solution, epitopes were demasked by Cell Conditioning 1 reagent and DAB staining was detected using UltraView Universal DAB Detection Kit or OptiView DAB IHC Detection Kit (all Roche). Following antibodies were detected: anti-SOX2 (#ab92494, Abcam), anti-OCT4 (#ab19857, Abcam), anti-NANOG (#ab109250, Abcam), anti-KLF4 (#ab215036, Abcam), anti-c-MYC (#ab32072, Abcam), anti-p53 (#05278775001, Roche), anti-MDM2 (#113-0230, Zytomed-Systems, Berlin, Germany), anti-Ki-67 (#Ki681C01, DCS, Hamburg, Germany). Antibody dilution, detection conditions and positive controls are detailed in Supplementary Table 4.

Immunostained slides were evaluated by experienced pathologist and scanned by motorized widefield microscope Zeiss AxioImager.Z2-ZEN with color camera AxioCam 208 using ZEN Blue software (Zeiss, Praha, Czech republic). QuPath software [19] was used to detect cell nuclei, classify tumor and non-tumor cells (machine learning-based classifiers were trained by experienced pathologist) and to perform DAB staining intensity analysis (machine learning-based intensity classifiers were trained on positive control tissues). The immunoreactivity of tumor cells was graded as none (–), weak (+), medium (++), and strong (+++). For each of the detected proteins, histoscores

were calculated as follows: 3×% of strongly positive cells + 2×% of medium positive cells + 1×% of weakly positive cells.

2.13. Statistical analysis

All statistical analyses were calculated from at least three biological replicates (details in figure legends) using GraphPad Prism 8.0.2 software. Individual data points in bar graphs represent independent biological replicates. Unpaired one/two-tailed Welch's t-test was performed for comparison between two groups. Multiple group comparison was analyzed using one-way ANOVA with Welch's correction followed by post-hoc Dunnett's test. Spearman correlation coefficient was determined for correlation analyses. Kaplan-Meier analyses were evaluated using Mantel-Cox test. Differences in sphere-forming frequency calculated by ELDA software and frequency of initial metastatic tumors were assessed by Chi-square test. p values < 0.05 were considered statistically significant; $^{*}p<0.05$, $^{**}p<0.01$, $^{***}p<0.001$.

3. RESULTS

3.1. SOX2 expression and dysregulated p53 pathway characterize tumorigenic stem-like sarcoma cells with aggressive growth *in vivo*

To test whether deregulation of the p53 pathway is connected with tumorigenic potential and stem-like traits of pediatric sarcomas, we first screened for the expression of canonical stemness-associated TFs: SOX2, OCT4, NANOG, KLF4, and c-MYC, together with p53 and MDM family proteins in a panel of 32 patient-derived and four established OS, RMS and ES cell lines (**Fig. 1a**, **S1**). From these proteins, p63, p73 and MDMX showed no significant expression heterogeneity, and thus were excluded from further analyses (**Fig. S2**). Based on the expression of stemness-associated TFs, we calculated stemness index (SI) of each sarcoma cell line (detailed formula in Methods) and used it as a classifier potentially reflecting stem-like capacity of sarcoma cells. We first identified SI^{high} (upper quartile SI) and SI^{low} (lower quartile SI) models in each subgroup of the patient-derived cell lines and then aligned established cell lines accordingly (**Fig. 1b**).

Testing SI^{high} and SI^{ow} sarcoma models *in vivo* revealed SI as a good predictor of tumorigenicity in immunodeficient NSG mice, which is still considered the most important hallmark of cancer stemness [20]. Only SI^{high} sarcoma cell lines (7/9 tested) were found to form xenograft tumors in mice while all

SI^{low} cell lines (0/9 tested) were non-tumorigenic (**Fig. 1b**). Notably, sarcoma models with the highest SI rapidly initiated very aggressive tumors whereas the only two SI^{high} cell lines that did not form tumors in mice showed absolute SI values comparable to those of non-tumorigenic SI^{low} counterparts (**Fig. 1b,c**). These results suggested that the most differentially expressed stemness-associated TFs might be key for the observed association between SI and tumorigenicity. In line with this, correlation analysis revealed that the tumorigenic capacity was strongly associated with levels of SOX2, and partially of OCT4 and NANOG (detected only in ES) (**Fig. 1d, S3**).

Importantly, tumorigenic SI^{high} models showed either markedly upregulated or downregulated levels of p53 relative to its median expression across all cell lines (**Fig. 1e**). Comparing SI^{high} models with the rest of the cell lines revealed that dysregulation of the p53 pathway is significantly associated with cancer stemness of pediatric sarcoma cells (**Fig. 1f**). Interestingly, although the established MNNG/HOS and RD tumorigenic cell lines both express mut-p53, no mutations in the *TP53* gene were identified by NGS in the SI^{high} and SI^{low} patient-derived sarcoma cell lines (**Fig. 1b**), suggesting different mechanisms of deregulated p53 activity were involved. Collectively, these data indicated an association between cancer stemness and p53 deregulation that might underly aggressive sarcoma cell phenotype.

We also asked whether SI established for the patient-derived cell lines could serve as a predictor of clinical outcomes. However, survival analysis revealed that the cell line-based SI, although informative of the stem-like phenotype of the model itself, is not suitable for patient outcome prediction and should be interpreted with great caution in that regard (**Fig. S4**). Of note, expression of all TFs and selected p53 pathway proteins was also evaluated at mRNA level, but a significantly less stable expression of individual transcripts was detected between biological replicates (**Fig. S5a**). Indeed, no association was then found between transcriptome data and tumorigenicity (**Fig. S5b**), which underpins the importance of analyzing expression levels of the encoded proteins directly to obtain proper insights into their roles in sarcomagenesis.

The tumor initiation in animal models is long known to select aggressive cancer clones which have the highest potential to form tumors *in vivo* [21] To analyze sarcoma phenotypes that are selected *in vivo*, xenografts obtained during the initial tumorigenicity assays in our study were processed and assembled into a self-constructed tissue microarray (TMA) and assessed by IHC (**Fig.**

2a,d). Following the evaluation by experienced pathologist, all slides were subjected to whole-slide scanning (**Fig. S6–9**) and computational image analysis using QuPath software, which allowed us to perform high-throughput quantitative expression analysis at the level of individual sarcoma cells using machine learning classifiers (**Fig. 2b**, **S10a,** for detailed results see **Fig. S11, S12**). This unbiased in-depth analysis revealed the same expression trends but provided higher sensitivity compared with the manual readout by pathologist (**Fig. 2c**, **S10b,** for detailed results see **Fig. S13**).

Of the examined proteins, IHC analyses revealed that majority of sarcoma xenografts maintained high expression of SOX2 but they generally lost OCT4 and NANOG expression, indicating the crucial role of SOX2 in sarcomagenesis (**Fig. 2b,c**). Moreover, abundant expression or a complete absence of p53 was observed in all of the analyzed sarcoma xenograft tissues (**Fig. 2b,c**). An interesting phenotypic switch was observed in the case of OS model OSA-13 with the complete absence of p53 expression, where KLF4 upregulation likely compensated for the loss of SOX2 expression.

3.2. SOX2 knockdown reduces sarcosphere formation capacity in the context of mut-p53

Our results linked stemness-associated TF SOX2 and dysregulated p53 pathway with aggressive stem-like phenotype of pediatric sarcoma cells. We therefore sought to elucidate whether different p53 background (mut-p53 vs wt-p53) affects how SOX2 contributes to sarcoma stemness. For this, we established single-cell clones with stable shRNA-mediated knockdown of SOX2 (shSOX2) derived from mut-p53 MNNG/HOS and wt-p53 ESFT-15 cells (**Fig. 3a,b**). Immunoblot analyses revealed that viable clones with inhibited SOX2 expression showed partial increase in NANOG expression and marked upregulation of KLF4 in MNNG/HOS and ESFT-15, respectively (**Fig. 3a**, **S14a**), indicating possible compensation of stem-like phenotype in the isolated single-cell clones. These findings are in accordance with the phenotypic switch observed in sarcoma xenografts, where KLF4 was likely compensating tumor-initiating capacity of OS patient-derived OSA-13 cells (**Fig. 2b**). Upregulation of *KLF4* in ESFT-15-shSOX2 cells was also detected at the mRNA level (**Fig. 3b**), together with an increase in *OCT4* and *NANOG* and a decrease in *MYC* transcripts, although these did not result in a significant change at protein levels (**Fig. 3a,b**, **S14a,b**).

To assess whether downregulation of SOX2 expression affects stemness of sarcoma cells in a p53 status-dependent manner, both shSOX2 and shRNA control (shCtrl) clones were subjected to sphere formation assay as the most comprehensive functional assay of cancer stem cell phenotype *in*

vitro. Unlike wt-p53 ESFT-15-shSOX2 cells, MNNG/HOS SOX2-knockdown clones carrying mut-p53 showed significantly reduced sphere-initiating capacity compared with their shCtrl counterparts (**Fig. 3c,d**). In line with the later tumor onset observed *in vivo* (**Fig. 1c**), wt-p53 ESFT-15-shCtrl cells also formed markedly less spheres compared with MNNG/HOS-shCtrl clones with mut-p53 (**Fig. 3c**). These results indicate that *TP53* mutation is an important step towards development of fully aggressive stem-like phenotype of sarcoma cells and further synergizes with the upregulation of stemness-associated TF SOX2.

3.3. Restoring p53 activity selectively induces cell death in aggressive stem-like Ewing's sarcoma cells

Mutations and other deregulations in the p53 pathway are associated with poor outcomes in pediatric sarcoma patients [1]. As our data pointed to the association of deregulated p53 with sarcoma stemness, we next asked whether p53 reactivation might selectively target stem-like sarcoma cells and impair their viability. Given the wt-p53 status of the patient-derived cell lines in this study, two compounds with essentially different mechanism of action–a dual inhibitor of MDM2/MDMX, RO-5963 [22], and a control mut-p53 reactivator, PRIMA-1^{MET} [23]–were tested in paired SI^{high} and SI^{low} cell lines from each of the sarcoma subgroups. Out of the SI^{high} and SI^{low} pairs tested, differential sensitivity to the p53 reactivation was observed only in the ES pair (**Fig. 4a**) where aggressive tumorigenic ESFT-15 cells showed markedly elevated p53 expression (indicating impaired p53 activity) compared with the non-tumorigenic ESFT-27 cells (**Fig. 1a**). SI^{high} ESFT-15 cells responded to ~40-fold lower concentrations of RO-5963 (absolute IC_{50} values 1.5 µM vs 56.4 µM) than SI^{low} ESFT-27 cells (**Fig. 4a**). Not surprisingly, when compared with results in healthy human fibroblast cells (**Fig. 4b**), treatment with PRIMA-1^{MET} designed to target mut-p53 did not show selective effects in the ES pair (**Fig. 4a**).

To further elucidate how p53 reactivation affects stem-like phenotype of sarcoma cells, we analyzed effects of RO-5963 in sensitive tumorigenic ESFT-15 cells. Interestingly, similarly to PRIMA-1^{MET}, RO-5963 treatment did not significantly alter the expression of neither of the examined stemness-associated TFs (**Fig. 4c**,**d**), suggesting that the selective antiproliferative effects of RO-5963 observed in SI^{high} ES cells are unlikely mediated by induced differentiation. To elucidate the underlying mechanism, we probed for p53, MDM2 and cleaved caspase-3 in ESFT-15 cells and control healthy fibroblasts treated with increasing concentrations (folds of IC_{50} values) of the drugs (**Fig. 5a,b**). Unlike

PRIMA-1^{MET}, inhibition of MDM2/MDMX-p53 interaction by RO-5963 led to p53 upregulation and induced apoptosis in ESFT-15 cells, as marked by dose-dependent increase cleaved caspase-3 levels (**Fig. 5a,b**). At least partial upregulation of p53 was detected also in both fibroblast cell lines; however, the induction of cleaved caspase-3 was either not detected or limited. Indeed, flow cytometry confirmed that RO-5963 treatment markedly induces cell death in SI^{high} ES cells while its cytotoxic effects on healthy fibroblasts were not dose-dependent and remained limited even at the highest concentration of the drug: 58.3 ± 2.6% vs. 4.8 ± 0.3% and 7.5 ± 1.9% (ESFT-15 vs. NDF-3 and NDF-2; **Fig. 5c,d**).

3.4. p53 associates with SOX2 expression in ES and is frequently positive in initially metastatic sarcomas

To assess the clinical relevance of the identified link between stemness expression signature and deregulated p53 pathway, we next performed IHC in a cohort of tumor tissues from 91 pediatric sarcoma patients. Altogether, 38 OS, 31 RMS and 41 ES tumor samples were stained and evaluated by experienced pathologist for the expression of p53, SOX2 and KLF4, which were found crucially involved in sarcoma initiation in our models. Interestingly, this analysis revealed a predominant expression of only one of the selected stemness-associated TFs in OS and ES. While KLF4 was almost exclusively expressed in OS tissues (28/38), SOX2 was not detected in any of the OS samples (**Fig 6a**). Conversely, upregulated SOX2 but not KLF4 was prevalent in ES tissues (12/41 vs. 1/41) (**Fig 6a**). SOX2 (4/31) and KLF4 (10/31) positivity without marked overexpression of one of these factors was observed in RMS samples (**Fig 6a**).

When correlated with the p53 expression, KLF4 did not associate with p53 positivity in OS samples (**Fig. 6b**). However, SOX2 was detected only in ES tissues concurrently overexpressing p53 (**Fig 6b,c**), further supporting our findings that suggest p53 deregulation as an important promoter of sarcoma stemness. To address whether SOX2, KLF4 and/or dysregulated expression of p53 potentially present a clinically useful prognostic biomarkers in our pediatric sarcoma cohort, correlation with clinicopathological data and survival analyses were performed using only samples from primary biopsies (n=91). This revealed that in OS cohort, metastases at the time of diagnosis were observed only in patients with KLF4 positive tumors (**Fig 6d**). Moreover, irrespective of the p53 levels, KLF4 positivity indicated a trend towards worse survival in OS patients (**Fig 6e**). High SOX2 expression was

recently suggested as an independent biomarker of poor prognosis in ES [24]. To analyze the prognostic significance of SOX2 in our ES cohort, we therefore applied a matching histoscore-based dichotomization: $SOX2^{low}$ (histoscore ≤45) and $SOX2^{high}$ (histoscore >45). Strikingly, this analysis did not show any correlation between the high SOX2 expression levels and presence of initial metastases (**Fig 6f**) or significant difference in survival rates of ES patients (**Fig 6g**).

In contrast, p53 positivity was significantly more prevalent in sarcoma patients with initial metastases (**Fig 6h**). Intriguingly, a trend of improved overall survival ($p = 0.09$) was observed in metastatic sarcomas positive for p53 (**Fig 6i**), suggesting that the absence of p53 expression in the context of already metastatic disease might be connected with the most unfavorable sarcoma prognosis.

Collectively, our results indicate that KLF4, SOX2 and p53 have rather limited prognostic power to serve as independent biomarkers of clinical outcomes in pediatric sarcomas. However, p53 positive staining significantly associates with metastatic tumors, which supports our experimental findings and points to the dysregulated p53 pathway as a clinically relevant target for therapies restoring wt-p53 function in aggressive sarcomas.

4. DISCUSSION

Pediatric sarcomas remain highly malignant tumors with unmet clinical needs. Previously, our group and others provided evidence linking the aggressive behavior of sarcoma cells to the cancer stem cell phenotype [9,10,25–27]. However, the primary determinants of sarcoma stemness and, more crucially, their clinical relevance, have remained poorly understood. In this study, we utilized an extensive panel of pediatric sarcoma models and tissue samples to explore whether deregulations of p53, recently identified regulator of stemness [1,28], are connected with stem-like phenotype of sarcoma cells. We show that altered p53 function associates with sarcoma stemness and aggressivity, and therefore might be exploited for developing novel therapies for at least some of the pediatric sarcomas refractory to available treatments.

While previous studies suggested numerous markers of sarcoma stemness [3,5–7], recent findings already emphasized that the primary focus should be directed towards investigating the role of

core stemness-associated TFs [9]. Indeed, estimating the stem-like potential based on the newly introduced SI, which reflects differential expression of stemness-associated TFs, proved to be a valuable predictor for the tumorigenicity of sarcoma cells in this study. Our initial screening highlighted SOX2 as a major marker of sarcoma stemness. Following analysis revealed that only cells expressing SOX2 or KLF4 were prevalent in sarcoma xenografts. The expression of OCT4 and/or NANOG detected in sarcoma cells *in vitro* was markedly suppressed or absent *in vivo*, which contradicts the previously suggested role of these TFs in sarcoma tumorigenicity [6,7,27]. Notably, our observations of almost exclusive KLF4 expression in OS xenografts with the absence of SOX2 were further corroborated by IHC analyses of human OS tissues. Consistent with experimental studies that indicated KLF4 as a promoter of stemness and metastasis in OS [13,29–31], we identified abundant KLF4 positivity associated with a trend towards worse survival in our OS cohort, suggesting KLF4 rather than SOX2 as a clinically relevant oncoprotein in OS. On the contrary, SOX2 dominated in ES tumors and was exclusively expressed in p53 positive cases. SOX2 has been recently reported as an independent marker of poor prognosis in ES [24] and sarcomas in general [26]. However, our study questions this prognostic utility, as we did not find any association between SOX2 expression and survival of ES patients. High expression of KLF4 and SOX2 identified in respective sarcoma subtypes is in agreement with previous studies [31,32].

Alteration of p53 has been suggested as an important promoter of sarcomagenesis in rodents and mesenchymal stem cell-derived models [33–36]. In line with these findings, our data obtained in a large panel of sarcoma cell lines revealed that high SI and enhanced tumorigenicity of sarcoma cells is associated with *TP53* mutations and other p53 pathway deregulations. This was further substantiated by the prevalent p53 positivity found in sarcoma tissues of patients with early metastatic disease. However, p53 expression failed to discriminate sarcoma patients with poor outcomes, adding to the contradictory results of other studies investigating the prognostic value of p53 in sarcoma patients [37–41]. Interestingly, none of our SI^{high} or SI^{low} patient-derived sarcoma cell lines carried mutation in *TP53*. This observation, especially in case of OS, is in contrast with the previously reported p53 mutation rates [1] and demonstrates that in the case of p53 status assessment, simple analysis of *TP53* DNA sequence is not sufficient for evaluating the dysregulation of p53 function. Indeed, p53 activity may be suppressed by various protein-protein interactions, including not only the well-known MDM molecules

[42] but also specific oncoproteins, such as the EWS-FLI-1 oncoprotein which is important for ES development [43].

Standard p53 activity was determined as a crucial constraint of reprograming and maintenance of stemness in induced pluripotent stem cells [44]. Consistently, we observed that p53 deregulation is connected with the expression of core stemness factor SOX2 in ES tissues. Strikingly, knockdown of SOX2 limited but not completely suppressed stemness of mut-p53 sarcoma cells, suggesting that p53 alteration is important for development of fully stem-like phenotype in sarcomas. Moreover, after successful SOX2 knockdown, we observed upregulation of NANOG and KLF4 transcription factors (both associated with cancer stemness [45,46]) in MNNG/HOS and ESFT-15 cell lines, respectively. These outcomes contrast with expectations based on prior studies, which suggested that downregulation of SOX2 reduces NANOG expression [47] and decreases the stability of KLF4 [48].

Given the identified link between deregulated p53 and aggressive stem-like sarcoma phenotype, we explored p53 reactivation as a potential approach to target sarcoma stem cells. In our first-in-field experiments, we compared the effects of compounds targeting p53 pathway on paired OS, RMS and ES cell lines with significantly different SI, and thus tumorigenic potential. By this approach, we demonstrated that SI^{high} tumorigenic ES cells exhibited higher sensitivity to p53 reactivation, in contrast to their SI^{low} counterparts. Inhibiting MDM2/MDMX-p53 interaction effectively induced p53 and apoptosis in stem-like ES cells carrying wt-p53 (present in a majority of ES [1]). RO-5963 upregulated levels of p53 protein at least partially in both ESFT-15 and fibroblasts, while markedly increased cell death only in tumorigenic SI^{high} cell line without significant effect on healthy fibroblasts, offering a potentially promising therapeutic window. Consistently, RO-5963 also previously proved its p53 reactivating potential connected with activation of apoptosis in OS cells with intact *TP53* [22]. Our results demonstrate that restriction of inhibitory binding of MDM2/MDMX to p53 represents a suitable approach to target aggressive ES.

In conclusion, our findings suggest that there is a strong association between p53 pathway deregulations, enhanced stemness-related transcription network (marked by SOX2 or KLF4 expression) and aggressive character of sarcoma cells. Clinically, alteration of p53 expression proved to be prevalent in metastatic sarcomas, providing a relevant target for reactivation therapies. We demonstrated that restoring p53 activity by MDM2/MDMX inhibition selectively and effectively targets

tumorigenic stem-like ES cells while causing no significant effect in healthy fibroblasts. Although further preclinical studies are needed to validate these results, we propose p53 reactivation as a promising strategy to treat refractory/metastatic p53-positive pediatric sarcomas.

FUNDING

This work was funded by the Ministry of Health of the Czech Republic (No. NU20J-07-00004).

ETHICS STATEMENT

This study was conducted in accordance with the Declaration of Helsinki and approved by the Research Ethics Committee of the Masaryk University (approval no. EKV-2019-051; granted on April 14, 2020). All human tumor tissues and noncommercial patient-derived sarcoma cell lines were obtained with written informed consent from patients or their legal guardians. Animal studies were approved by the Institutional Animal Care and Use Committee of the Masaryk University and registered by the Ministry of Education, Youth and Sports of the Czech Republic (ref. no. MSMT-4408/2016-6) as required by national legislation.

CREDIT AUTHORSHIP CONTRIBUTION STATEMENT

Lucie Curylova: Writing - original draft, Investigation, Methodology, Formal analysis, Visualization, Data curation. **Iva Staniczkova Zambo**: Investigation, Visualization, Writing - review & editing. **Jakub Neradil**: Investigation, Writing - review & editing. **Michal Kyr**: Data curation, Formal analysis, Writing - review & editing. **Nicola Jurackova**: Methodology, Investigation. **Sarka Pavlova**: Investigation. **Kristyna Polaskova**: Data curation. **Peter Mudry**: Resources. **Jaroslav Sterba**: Resources. **Renata Veselska**: Resources, Funding acquisition. **Jan Skoda**: Conceptualization, Writing – original draft, Formal analysis, Visualization, Funding acquisition, Supervision, Project administration. All authors read and approved the final version of the manuscript.

DECLARATION OF COMPETING INTEREST

The authors declare that they have no known competing financial interests or personal relationships that could have appeared to influence the work reported in this paper.

ACKNOWLEDGEMENTS

LC was supported by the Brno Ph.D. Talent Scholarship funded by the Brno City Municipality. JN, KP, RV and JS (Jan Skoda) acknowledge the project National Institute for Cancer Research (Programme EXCELES, ID Project No. LX22NPO5102)—Funded by the European Union—Next Generation EU. SP acknowledges the conceptual development of research organization (FNBr 65269705) provided by the Ministry of Health of the Czech Republic. The authors thank Dr. Jan Verner and Johana Marešová for their skillful technical assistance, and Dr. Tomáš Bárta (Department of Histology and Embryology, Faculty of Medicine, Masaryk University) for providing normal fibroblast cell lines.

REFERENCES

[1] L. Curylova, H. Ramos, L. Saraiva, J. Skoda, Noncanonical roles of p53 in cancer stemness and their implications in sarcomas, Cancer Lett. 525 (2022) 131–145. https://doi.org/10.1016/j.canlet.2021.10.037.

[2] E. Thoenen, A. Curl, T. Iwakuma, TP53 in bone and soft tissue sarcomas, Pharmacol. Ther. 202 (2019) 149–164. https://doi.org/10.1016/j.pharmthera.2019.06.010.

[3] J. Skoda, R. Veselska, Cancer stem cells in sarcomas: Getting to the stemness core, Biochim. Biophys. Acta Gen. Subj. 1862 (2018) 2134–2139. https://doi.org/10.1016/j.bbagen.2018.07.006.

[4] S.M. Perkins, E.T. Shinohara, T. DeWees, H. Frangoul, Outcome for children with metastatic solid tumors over the last four decades, PloS One 9 (2014) e100396. https://doi.org/10.1371/journal.pone.0100396.

[5] V. Tirino, V. Desiderio, R. d'Aquino, F. De Francesco, G. Pirozzi, A. Graziano, U. Galderisi, C. Cavaliere, A. De Rosa, G. Papaccio, A. Giordano, Detection and characterization of CD133+ cancer stem cells in human solid tumours, PloS One 3 (2008) e3469. https://doi.org/10.1371/journal.pone.0003469.

[6] M.-L. Suvà, N. Riggi, J.-C. Stehle, K. Baumer, S. Tercier, J.-M. Joseph, D. Suvà, V. Clément, P. Provero, L. Cironi, M.-C. Osterheld, L. Guillou, I. Stamenkovic, Identification of cancer stem cells in Ewing's sarcoma, Cancer Res. 69 (2009) 1776–1781. https://doi.org/10.1158/0008-5472.CAN-08-2242.

[7] L. Wang, P. Park, H. Zhang, F. La Marca, C.-Y. Lin, Prospective identification of tumorigenic osteosarcoma cancer stem cells in OS99-1 cells based on high aldehyde dehydrogenase activity, Int. J. Cancer 128 (2011) 294–303. https://doi.org/10.1002/ijc.25331.

[8] J.-C. Yeo, H.-H. Ng, The transcriptional regulation of pluripotency, Cell Res. 23 (2013) 20–32. https://doi.org/10.1038/cr.2012.172.

[9] J. Skoda, A. Nunukova, T. Loja, I. Zambo, J. Neradil, P. Mudry, K. Zitterbart, M. Hermanova, A. Hampl, J. Sterba, R. Veselska, Cancer stem cell markers in pediatric sarcomas: Sox2 is associated with tumorigenicity in immunodeficient mice, Tumour Biol. 37 (2016) 9535–9548. https://doi.org/10.1007/s13277-016-4837-0.

[10] G. Maurizi, N. Verma, A. Gadi, A. Mansukhani, C. Basilico, Sox2 is required for tumor development and cancer cell proliferation in osteosarcoma, Oncogene 37 (2018) 4626–4632. https://doi.org/10.1038/s41388-018-0292-2.

[11] K.C. Genadry, S. Pietrobono, R. Rota, C.M. Linardic, Soft Tissue Sarcoma Cancer Stem Cells: An Overview, Front. Oncol. 8 (2018) 475. https://doi.org/10.3389/fonc.2018.00475.

[12] C.N. Amaya, B.A. Bryan, Enrichment of the embryonic stem cell reprogramming factors Oct4, Nanog, Myc, and Sox2 in benign and malignant vascular tumors, BMC Clin. Pathol. 15 (2015) 18. https://doi.org/10.1186/s12907-015-0018-0.

[13] S.R. Martins-Neves, W.E. Corver, D.I. Paiva-Oliveira, B.E.W.M. van den Akker, I.H. Briaire-de-Bruijn, J.V.M.G. Bovée, C.M.F. Gomes, A.-M. Cleton-Jansen, Osteosarcoma Stem Cells Have Active Wnt/β-catenin and Overexpress SOX2 and KLF4, J. Cell. Physiol. 231 (2016) 876–886. https://doi.org/10.1002/jcp.25179.

[14] A. Huyghe, A. Trajkova, F. Lavial, Cellular plasticity in reprogramming, rejuvenation and tumorigenesis: a pioneer TF perspective, Trends Cell Biol. (2023) S0962-8924(23)00157–5. https://doi.org/10.1016/j.tcb.2023.07.013.

[15] D.J. Olivos, L.D. Mayo, Emerging Non-Canonical Functions and Regulation by p53: p53 and Stemness, Int. J. Mol. Sci. 17 (2016). https://doi.org/10.3390/ijms17121982.

[16] P. Kameneva, V.I. Melnikova, M.E. Kastriti, A. Kurtova, E. Kryukov, A. Murtazina, L. Faure, I. Poverennaya, A.V. Artemov, T.S. Kalinina, N.V. Kudryashov, M. Bader, J. Skoda, P. Chlapek, L. Curylova, L. Sourada, J. Neradil, M. Tesarova, M. Pasqualetti, P. Gaspar, V.D. Yakushov, B.I. Sheftel, T. Zikmund, J. Kaiser, K. Fried, N. Alenina, E.E. Voronezhskaya, I. Adameyko, Serotonin limits generation of chromaffin cells during adrenal organ development, Nat. Commun. 13 (2022) 2901. https://doi.org/10.1038/s41467-022-30438-w.

[17] J. Malcikova, S. Pavlova, B. Kunt Vonkova, L. Radova, K. Plevova, J. Kotaskova, K. Pal, B. Dvorackova, M. Zenatova, J. Hynst, E. Ondrouskova, A. Panovska, Y. Brychtova, K. Zavacka, B. Tichy, N. Tom, J. Mayer, M. Doubek, S. Pospisilova, Low-burden TP53 mutations in CLL: clinical impact and clonal evolution within the context of different treatment options, Blood 138 (2021) 2670–2685. https://doi.org/10.1182/blood.2020009530.

[18] Y. Hu, G.K. Smyth, ELDA: extreme limiting dilution analysis for comparing depleted and enriched populations in stem cell and other assays, J. Immunol. Methods 347 (2009) 70–78. https://doi.org/10.1016/j.jim.2009.06.008.

[19] P. Bankhead, M.B. Loughrey, J.A. Fernández, Y. Dombrowski, D.G. McArt, P.D. Dunne, S. McQuaid, R.T. Gray, L.J. Murray, H.G. Coleman, J.A. James, M. Salto-Tellez, P.W. Hamilton, QuPath: Open source software for digital pathology image analysis, Sci. Rep. 7 (2017) 16878. https://doi.org/10.1038/s41598-017-17204-5.

[20] J.D. Lathia, H. Liu, Overview of Cancer Stem Cells and Stemness for Community Oncologists, Target. Oncol. 12 (2017) 387–399. https://doi.org/10.1007/s11523-017-0508-3.

[21] E. Halachmi, I.P. Witz, Differential tumorigenicity of 3T3 cells transformed in vitro with polyoma virus and in vivo selection for high tumorigenicity, Cancer Res. 49 (1989) 2383–2389.

[22] B. Graves, T. Thompson, M. Xia, C. Janson, C. Lukacs, D. Deo, P. Di Lello, D. Fry, C. Garvie, K.-S. Huang, L. Gao, C. Tovar, A. Lovey, J. Wanner, L.T. Vassilev, Activation of the p53 pathway by small-molecule-induced MDM2 and MDMX dimerization, Proc. Natl. Acad. Sci. U. S. A. 109 (2012) 11788–11793. https://doi.org/10.1073/pnas.1203789109.

[23] V.J.N. Bykov, N. Zache, H. Stridh, J. Westman, J. Bergman, G. Selivanova, K.G. Wiman, PRIMA-1(MET) synergizes with cisplatin to induce tumor cell apoptosis, Oncogene 24 (2005) 3484–3491. https://doi.org/10.1038/sj.onc.1208419.

[24] G. Sannino, A. Marchetto, A. Ranft, S. Jabar, C. Zacherl, R. Alba-Rubio, S. Stein, F.S. Wehweck, M.M. Kiran, T.L.B. Hölting, J. Musa, L. Romero-Pérez, F. Cidre-Aranaz, M.M.L. Knott, J. Li, H. Jürgens, A. Sastre, J. Alonso, W. Da Silveira, G. Hardiman, J.S. Gerke, M.F. Orth, W. Hartmann, T. Kirchner, S. Ohmura, U. Dirksen, T.G.P. Grünewald, Gene expression and immunohistochemical analyses identify SOX2 as major risk factor for overall survival and relapse in Ewing sarcoma patients, EBioMedicine 47 (2019) 156–162. https://doi.org/10.1016/j.ebiom.2019.08.002.

[25] U. Basu-Roy, E. Seo, L. Ramanathapuram, T.B. Rapp, J.A. Perry, S.H. Orkin, A. Mansukhani, C. Basilico, Sox2 maintains self renewal of tumor-initiating cells in osteosarcomas, Oncogene 31 (2012) 2270–2282. https://doi.org/10.1038/onc.2011.405.

[26] S.T. Menendez, V. Rey, L. Martinez-Cruzado, M.V. Gonzalez, A. Morales-Molina, L. Santos, V. Blanco, C. Alvarez, O. Estupiñan, E. Allonca, J.P. Rodrigo, J. García-Castro, J.M. Garcia-Pedrero, R. Rodriguez, SOX2 Expression and Transcriptional Activity Identifies a Subpopulation of Cancer Stem Cells in Sarcoma with Prognostic Implications, Cancers 12 (2020) 964. https://doi.org/10.3390/cancers12040964.

[27] D. Walter, S. Satheesha, P. Albrecht, B.C. Bornhauser, V. D'Alessandro, S.M. Oesch, H. Rehrauer, I. Leuschner, E. Koscielniak, C. Gengler, H. Moch, M. Bernasconi, F.K. Niggli, B.W. Schäfer, CWS Study Group, CD133 positive embryonal rhabdomyosarcoma stem-like cell population is enriched in rhabdospheres, PloS One 6 (2011) e19506. https://doi.org/10.1371/journal.pone.0019506.

[28] R. Aloni-Grinstein, Y. Shetzer, T. Kaufman, V. Rotter, p53: the barrier to cancer stem cell formation, FEBS Lett. 588 (2014) 2580–2589. https://doi.org/10.1016/j.febslet.2014.02.011.

[29] W.D. Pontius, E.S. Hong, Z.J. Faber, J. Gray, C.D. Peacock, I. Bayles, K. Lovrenert, D.H. Chin, B.E. Gryder, C.F. Bartels, P.C. Scacheri, Temporal chromatin accessibility changes define transcriptional states essential for osteosarcoma metastasis, Nat. Commun. 14 (2023) 7209. https://doi.org/10.1038/s41467-023-42656-x.

[30] Y. Li, M. Xian, B. Yang, M. Ying, Q. He, Inhibition of KLF4 by Statins Reverses Adriamycin-Induced Metastasis and Cancer Stemness in Osteosarcoma Cells, Stem Cell Rep. 8 (2017) 1617–1629. https://doi.org/10.1016/j.stemcr.2017.04.025.

[31] L. Zhang, L. Zhang, X. Xia, S. He, H. He, W. Zhao, Krüppel-like factor 4 promotes human osteosarcoma growth and metastasis via regulating CRYAB expression, Oncotarget 7 (2016) 30990–31000. https://doi.org/10.18632/oncotarget.8824.

[32] C. Ren, T. Ren, K. Yang, S. Wang, X. Bao, F. Zhang, W. Guo, Inhibition of SOX2 induces cell apoptosis and G1/S arrest in Ewing's sarcoma through the PI3K/Akt pathway, J. Exp. Clin. Cancer Res. 35 (2016) 44. https://doi.org/10.1186/s13046-016-0321-3.

[33] H. Li, X. Fan, R.C. Kovi, Y. Jo, B. Moquin, R. Konz, C. Stoicov, E. Kurt-Jones, S.R. Grossman, S. Lyle, A.B. Rogers, M. Montrose, J. Houghton, Spontaneous expression of embryonic factors and p53 point mutations in aged mesenchymal stem cells: a model of age-related tumorigenesis in mice, Cancer Res. 67 (2007) 10889–10898. https://doi.org/10.1158/0008-5472.CAN-07-2665.

[34] P.P. Lin, M.K. Pandey, F. Jin, A.K. Raymond, H. Akiyama, G. Lozano, Targeted mutation of p53 and Rb in mesenchymal cells of the limb bud produces sarcomas in mice, Carcinogenesis 30 (2009) 1789–1795. https://doi.org/10.1093/carcin/bgp180.

[35] R. Rubio, I. Gutierrez-Aranda, A.I. Sáez-Castillo, A. Labarga, M. Rosu-Myles, S. Gonzalez-Garcia, M.L. Toribio, P. Menendez, R. Rodriguez, The differentiation stage of p53-Rb-deficient bone marrow mesenchymal stem cells imposes the phenotype of in vivo sarcoma development, Oncogene 32 (2013) 4970–4980. https://doi.org/10.1038/onc.2012.507.

[36] R. van Boxtel, R.V. Kuiper, P.W. Toonen, S. van Heesch, R. Hermsen, A. de Bruin, E. Cuppen, Homozygous and heterozygous p53 knockout rats develop metastasizing sarcomas with high frequency, Am. J. Pathol. 179 (2011) 1616–1622. https://doi.org/10.1016/j.ajpath.2011.06.036.

[37] D. Yao, G.-H. Cai, J. Chen, R. Ling, S.-X. Wu, Y.-P. Li, Prognostic value of p53 alterations in human osteosarcoma: a meta analysis, Int. J. Clin. Exp. Pathol. 7 (2014) 6725–6733.

[38] J. Wu, A. Guo, Q. Li, D. Wang, Meta-analysis of clinical significance of p53 protein expression in patients with osteosarcoma, Future Oncol. 13 (2017) 1883–1891. https://doi.org/10.2217/fon-2017-0180.

[39] I. Leuschner, I. Langhans, R. Schmitz, D. Harms, A. Mattke, J. Treuner, Kiel Pediatric Tumor Registry and the German Cooperative Soft Tissue Sarcoma Study, p53 and mdm-2 expression in Rhabdomyosarcoma of childhood and adolescence: clinicopathologic study by the Kiel Pediatric Tumor Registry and the German Cooperative Soft Tissue Sarcoma Study, Pediatr. Dev. Pathol. 6 (2003) 128–136. https://doi.org/10.1007/s10024-001-0097-z.

[40] I. Ayan, O. Dŏgan, R. Kebudi, B. Bavbek, C. Alatli, S. Dervişoğlu, R. Dişçi, M. Demiryont, Immunohistochemical detection of p53 protein in rhabdomyosarcoma: association with clinicopathological features and outcome, J. Pediatr. Hematol. Oncol. 19 (1997) 48–53. https://doi.org/10.1097/00043426-199701000-00007.

[41] Y. Yang, T. Zhen, F. Zhang, S. Dai, L. Kang, Y. Liang, L. Xue, A. Han, p53 and hepatoma-derived growth factor expression and their clinicopathological association with Ewing family tumour, J. Clin. Pathol. 67 (2014) 235–242. https://doi.org/10.1136/jclinpath-2013-201705.

[42] Y. Haupt, R. Maya, A. Kazaz, M. Oren, Mdm2 promotes the rapid degradation of p53, Nature 387 (1997) 296–299. https://doi.org/10.1038/387296a0.

[43] Y. Li, K. Tanaka, X. Fan, F. Nakatani, X. Li, T. Nakamura, M. Takasaki, S. Yamamoto, Y. Iwamoto, Inhibition of the transcriptional function of p53 by EWS-Fli1 chimeric protein in Ewing Family Tumors, Cancer Lett. 294 (2010) 57–65. https://doi.org/10.1016/j.canlet.2010.01.022.

[44] X. Fu, S. Wu, B. Li, Y. Xu, J. Liu, Functions of p53 in pluripotent stem cells, Protein Cell 11 (2020) 71–78. https://doi.org/10.1007/s13238-019-00665-x.

[45] A. Liu, X. Yu, S. Liu, Pluripotency transcription factors and cancer stem cells: small genes make a big difference, Chin. J. Cancer 32 (2013) 483–487. https://doi.org/10.5732/cjc.012.10282.

[46] Z. Zeng, M. Fu, Y. Hu, Y. Wei, X. Wei, M. Luo, Regulation and signaling pathways in cancer stem cells: implications for targeted therapy for cancer, Mol. Cancer 22 (2023) 172. https://doi.org/10.1186/s12943-023-01877-w.

[47] H. Fong, K.A. Hohenstein, P.J. Donovan, Regulation of self-renewal and pluripotency by Sox2 in human embryonic stem cells, Stem Cells 26 (2008) 1931–1938. https://doi.org/10.1634/stemcells.2007-1002.

[48] N.K. Dhaliwal, L.E. Abatti, J.A. Mitchell, KLF4 protein stability regulated by interaction with pluripotency transcription factors overrides transcriptional control, Genes Dev. 33 (2019) 1069–1082. https://doi.org/10.1101/gad.324319.119.

FIGURE LEGENDS

Figure 1: Expression of SOX2, OCT4, and NANOG TFs and p53 deregulations *in vitro* associate with pediatric sarcoma tumorigenicity. a) Representative images of western blot analysis (biological n=3) of stemness-associated TFs SOX2, NANOG, OCT4, KLF4 and c-MYC and p53 pathway proteins, p53 and MDM2, in a panel of established and patient-derived OS, RMS and ES cell lines. Densitometric analysis is provided in Fig. S1. **b)** Heat maps (top) of the mean protein expression (n=3) of stemness-related TFs, p53 and MDM2. Cell lines of each sarcoma subgroup are aligned according to the calculated SI (middle). The scheme (bottom) illustrates the tumorigenicity of SI^{high} and SI^{low} cell lines assayed in NSG mice (n=3). **c)** Survival of xenograft mouse models (n=3 mice per cell line) reflecting tumor-initiating capacity and xenograft growth rates of the sarcoma cell lines tested. **d)** A significant positive correlation between the expression of SOX2, OCT4 and NANOG TFs and number of tumors formed by sarcoma cell lines in mice. **e)** Correlation between SI values and p53 protein level in individual cell lines relative to the mean expression of each sarcoma subtype. Note that all tumorigenic SI^{high} models exhibit deregulated p53 expression and fit within the upper or lower quartiles (indicated by dotted lines). **f)** p53 levels in SI^{high} models are significantly different compared to the rest of the sarcoma cell lines. Data are presented as mean ± SD. Statistical significance was determined by one-tailed Welch's t-test **(f)** and by Spearman correlation coefficient **(d)**, *p<0.05, **p<0.01, ***p<0.001.

Figure 2: Cells with high SOX2 or KLF4 and dysregulated p53 expression are prevalent in sarcoma xenografts. a) An overview of the in-house pipeline for TMA assembly followed by IHC staining and machine learning-assisted image analysis of the whole-slide scanned TMA sections. **b, c)** Staining intensity of p53 and stemness-related TFs assessed by computational analysis in QuPath software (**b**) or manual readout by experienced pathologist (**c**). Data shown as mean ± SD, biological n=3. **d)** Representative images of IHC detection of SOX2, KLF4 and p53 in xenograft tumors formed by the indicated cell lines or in positive control tissues (SOX2, fetal lungs; KLF4, seminoma; p53, tonsilla).

Figure 3: Knockdown of SOX2 expression is associated with downregulation of sphere-formation capacity in sarcoma cells with mut-p53. a) Representative western blot images (right) and densitometric analysis (left) of stemness-associated TFs, p53 and MDM2 in mut-p53 MNNG/HOS

and wt-p53 ESFT-15 clones with shRNA-mediated knockdown of SOX2 (shSOX2) compared with their scramble shRNA controls (shCtrl). Data presented as mean ± SD, biological n=3–4. Densitometric analysis of OCT4, c-MYC, and MDM2 proteins is provided in Fig. S10a. **b)** qPCR analysis of selected stemness-associated TFs in MNNG/HOS and ESFT-15 shSOX2 clones. Data are presented as mean ± SD, biological n=3, technical n=3. Analysis of remaining genes is provided in Fig. S10b. **c)** Sphere formation assay evaluating stem-like phenotype of MNNG/HOS and ESFT-15 sarcoma cells after SOX2 knockdown. Stem cell frequencies and probability were computed using ELDA software [18]. Data are shown as mean ± 95% confidence interval, biological n=3–4, technical n=5. **d)** Representative images of sarcospheres formed by shCtrl and shSOX2 clones of MNNG/HOS and ESFT-15 cell lines. All experiments were performed using single cell-derived clones (indicated by numbers). Statistical significance was determined by one-way ANOVA with Welch's correction followed by post-hoc Dunnett's test (**a, b**) or Chi-square pairwise test (**c**), *p<0.05, **p<0.01, ***p<0.001.

Figure 4: Stem-like Ewing's sarcoma cells are vulnerable to p53 reactivation. a) MTT cell viability assay of SI^{high} and SI^{low} OS, RMS and ES cell lines after 72-h treatment by RO-5963 or PRIMA-1^{MET}. Note that only cells derived from ES showed marked difference in sensitivity to re-activation of p53. Data are presented as mean ± SD, biological n=3–5, technical n=3–5. **b)** MTT cell viability assay of control healthy fibroblast cell lines after 72-h exposure to RO-5963 or PRIMA-1^{MET}. Data are presented as mean ± SD, biological n=3, technical n=3–5. **c, d)** Representative western blot images (**c**) and densitometric analysis (**d**) of stemness-associated TFs expression in aggressive ESFT-15 cells after 72-h treatment with RO-5963 or PRIMA-1^{MET}. Ctrl, DMSO treated control. Data shown as mean ± SD, biological n=3. Statistical significance was determined by one-way ANOVA with Welch's correction followed by post-hoc Dunnett's test, **p<0.01.

Figure 5: Inhibition of MDM2/MDMX-p53 interaction potently activates p53 pathway and induces cell death in aggressive Ewing's sarcoma cells without marked cytotoxicity in healthy fibroblasts. a, b) Representative western blot images (**a**) and densitometric analysis (**b**) of p53, MDM2 and cleaved caspase-3 expression in ESFT-15 ES cell line and healthy fibroblasts NDF-3 and NDF-2 after 72-h exposure to RO-5963 and PRIMA-1^{MET}. Data are presented as mean ± SD, biological n=3. **c)** Representative flow cytometry histograms showing marked difference in SYTOX Red-positive dead cells in ESFT-15 and fibroblast cell lines after 72-h exposure to $10\times IC_{50}$ (ESFT-15)

of RO-5963. **d)** Flow cytometry analysis of dead vs. live cells after 72-h treatment with p53 pathway targeting drugs, RO-5963 and PRIMA-1^{MET}. Data presented as mean ± SD, biological n=3-6. Ctrl, DMSO treated control. Statistical significance in was determined by one-way ANOVA with Welch's correction followed by post-hoc Dunnett's test (**b,d**), *p<0.05, **p<0.01, ***p<0.001.

Fig 6: p53 positivity associates with SOX2 expression in ES and is more prevalent in initially metastatic sarcomas. a) IHC analysis of SOX2 and KLF4 expression in OS, RMS and ES biopsies. **b)** Expression of KLF4 and SOX2 in p53-positive and p53-negative OS and ES tissues, respectively. Note that in ES, SOX2 was detected only in p53-positive biopsies. **c)** Representative images of SOX2 and p53 IHC analysis in ES tissue. **d)** Frequency of initial metastases in OS patients with KLF4-positive and KLF4-negative tumors. **e)** Kaplan-Meier analysis of OS patients stratified by KLF4 and p53 protein expression. **f)** Frequency of initial metastases in ES patients with SOX2^{high} and SOX2^{low} tumors. **g)** Kaplan-Meier analysis of ES patients stratified by SOX2 protein expression (cut-off for SOX2^{low} histoscore value was determined as ≤ 45). **h)** Frequency of initial metastases in pediatric sarcoma patients with p53-positive and p53-negative tumors, showing that p53 expression is associated with early metastatic disease. **i)** Kaplan-Meier analysis of sarcoma patients stratified by p53 protein expression and presence of initial metastases. M0, no metastatic events; M1, presence of initial metastases. Statistical significance was determined by Welch's t-test (**a, b**), Chi-square test (**d, f, h**) and Mantel-Cox test (**e, g, i**), *p<0.05, **p<0.01, ***p<0.001.

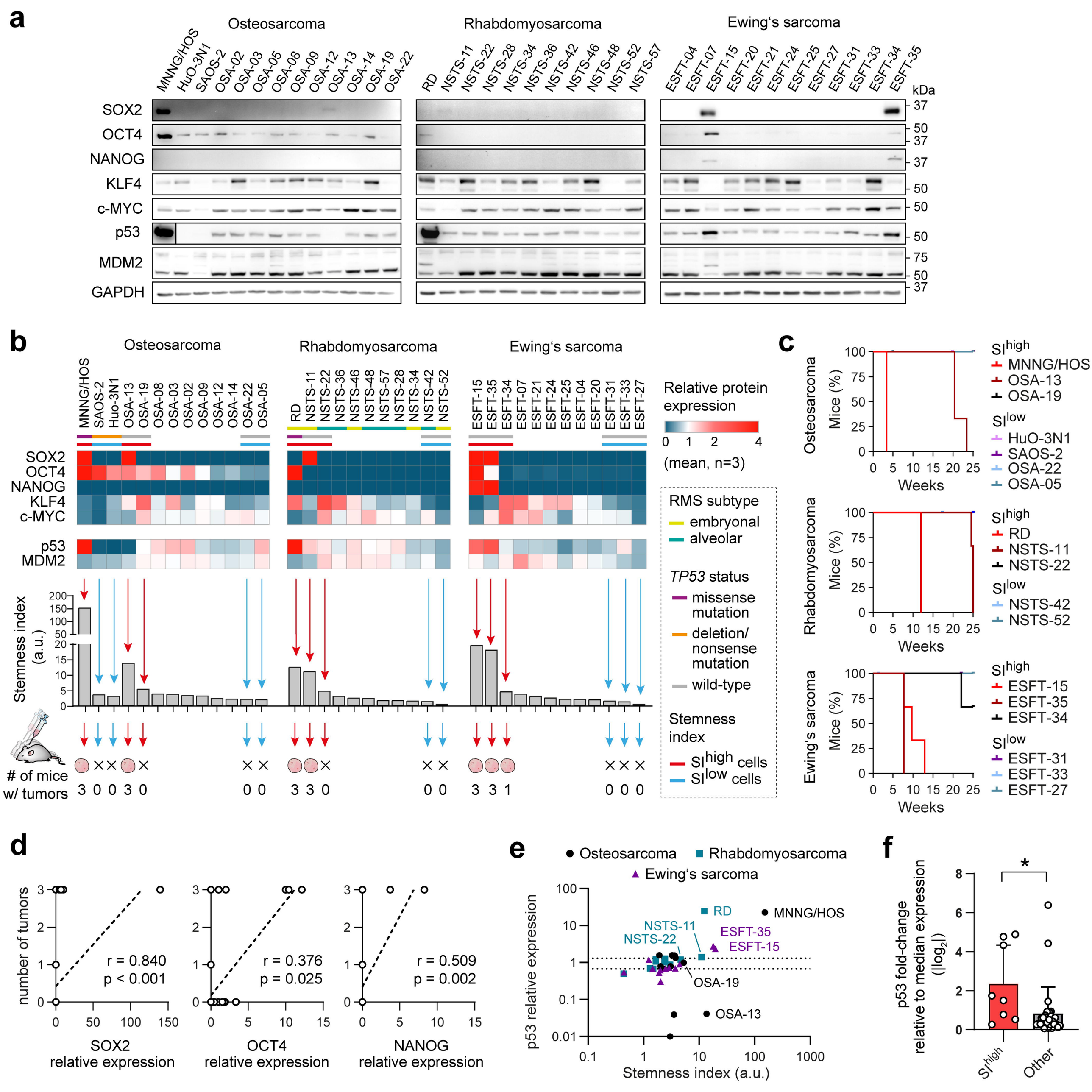
a
Osteosarcoma
Rhabdomyosarcoma
Ewing's sarcoma
MNNG/HOS
HuO-3N1
SAOS-2
OSA-02
OSA-03
OSA-05
OSA-08
OSA-09
OSA-12
OSA-13
OSA-14
OSA-19
OSA-22
RD
NSTS-11
NSTS-22
NSTS-28
NSTS-34
NSTS-36
NSTS-42
NSTS-46
NSTS-48
NSTS-52
NSTS-57
ESFT-04
ESFT-07
ESFT-15
ESFT-20
ESFT-21
ESFT-24
ESFT-25
ESFT-27
ESFT-31
ESFT-33
ESFT-34
ESFT-35
kDa
SOX2
OCT4
NANOG
KLF4
c-MYC
p53
MDM2
GAPDH
b
Osteosarcoma
Rhabdomyosarcoma
Ewing's sarcoma
Relative protein expression
(mean, n=3)
RMS subtype
embryonal
alveolar
TP53 status
missense mutation
deletion/ nonsense mutation
wild-type
Stemness index
SI high cells
SI low cells
Stemness index (a.u.)
# of mice w/ tumors
c
Osteosarcoma
Rhabdomyosarcoma
Ewing's sarcoma
Mice (%)
Weeks
SI high
MNNG/HOS
OSA-13
OSA-19
SI low
HuO-3N1
SAOS-2
OSA-22
OSA-05
RD
NSTS-11
NSTS-22
NSTS-42
NSTS-52
ESFT-15
ESFT-35
ESFT-34
ESFT-31
ESFT-33
ESFT-27
d
number of tumors
r = 0.840
p < 0.001
r = 0.376
p = 0.025
r = 0.509
p = 0.002
SOX2 relative expression
OCT4 relative expression
NANOG relative expression
e
Osteosarcoma
Rhabdomyosarcoma
Ewing's sarcoma
RD
MNNG/HOS
NSTS-11
NSTS-22
ESFT-35
ESFT-15
OSA-19
OSA-13
p53 relative expression
Stemness index (a.u.)
f
p53 fold-change relative to median expression (|log2|)
SI high
Other

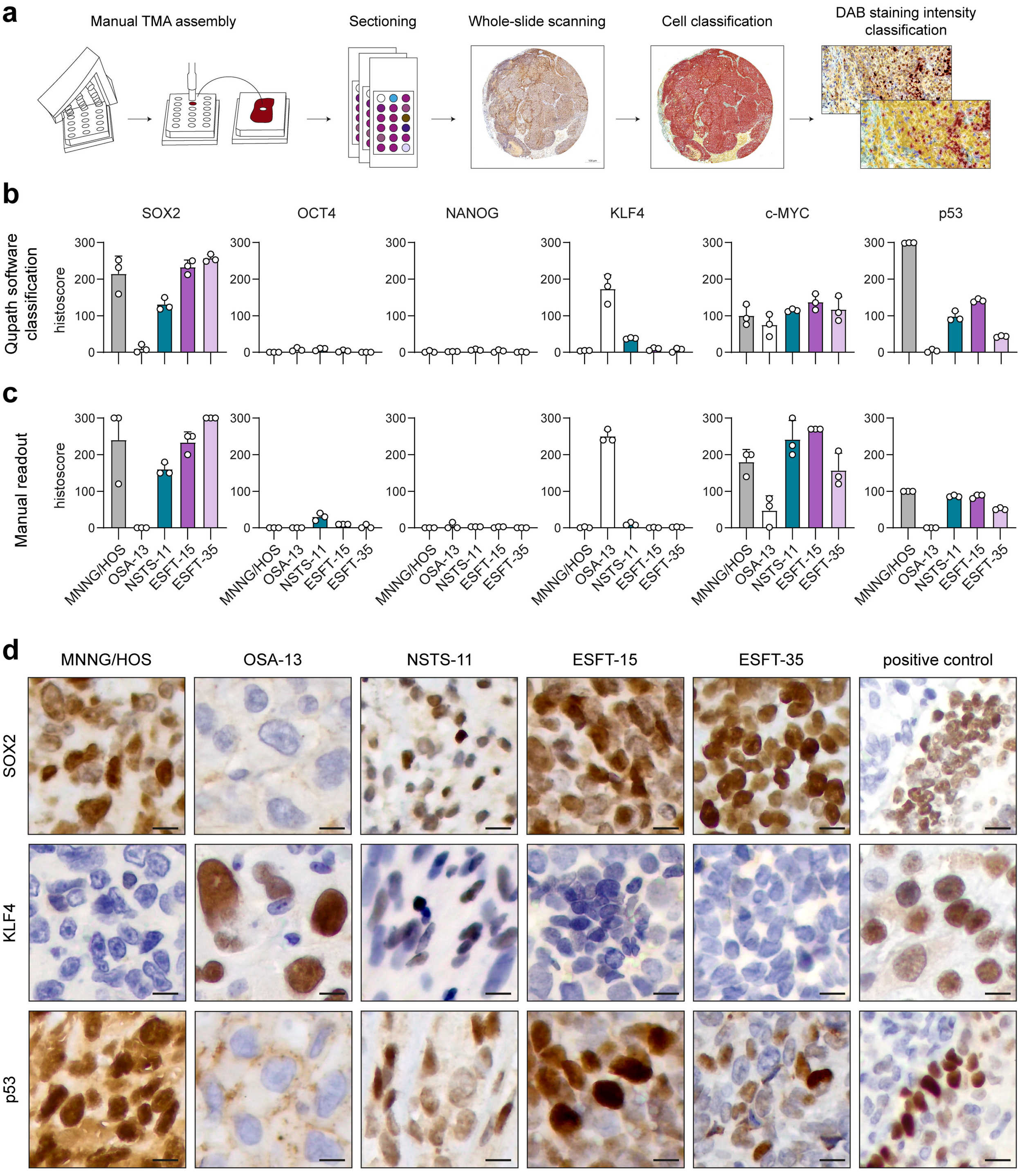
a
Manual TMA assembly
Sectioning
Whole-slide scanning
Cell classification
DAB staining intensity classification
b
SOX2
OCT4
NANOG
KLF4
c-MYC
p53
Qupath software classification
histoscore
c
Manual readout
histoscore
MNNG/HOS
OSA-13
NSTS-11
ESFT-15
ESFT-35
d
MNNG/HOS
OSA-13
NSTS-11
ESFT-15
ESFT-35
positive control
SOX2
KLF4
p53
10 µm

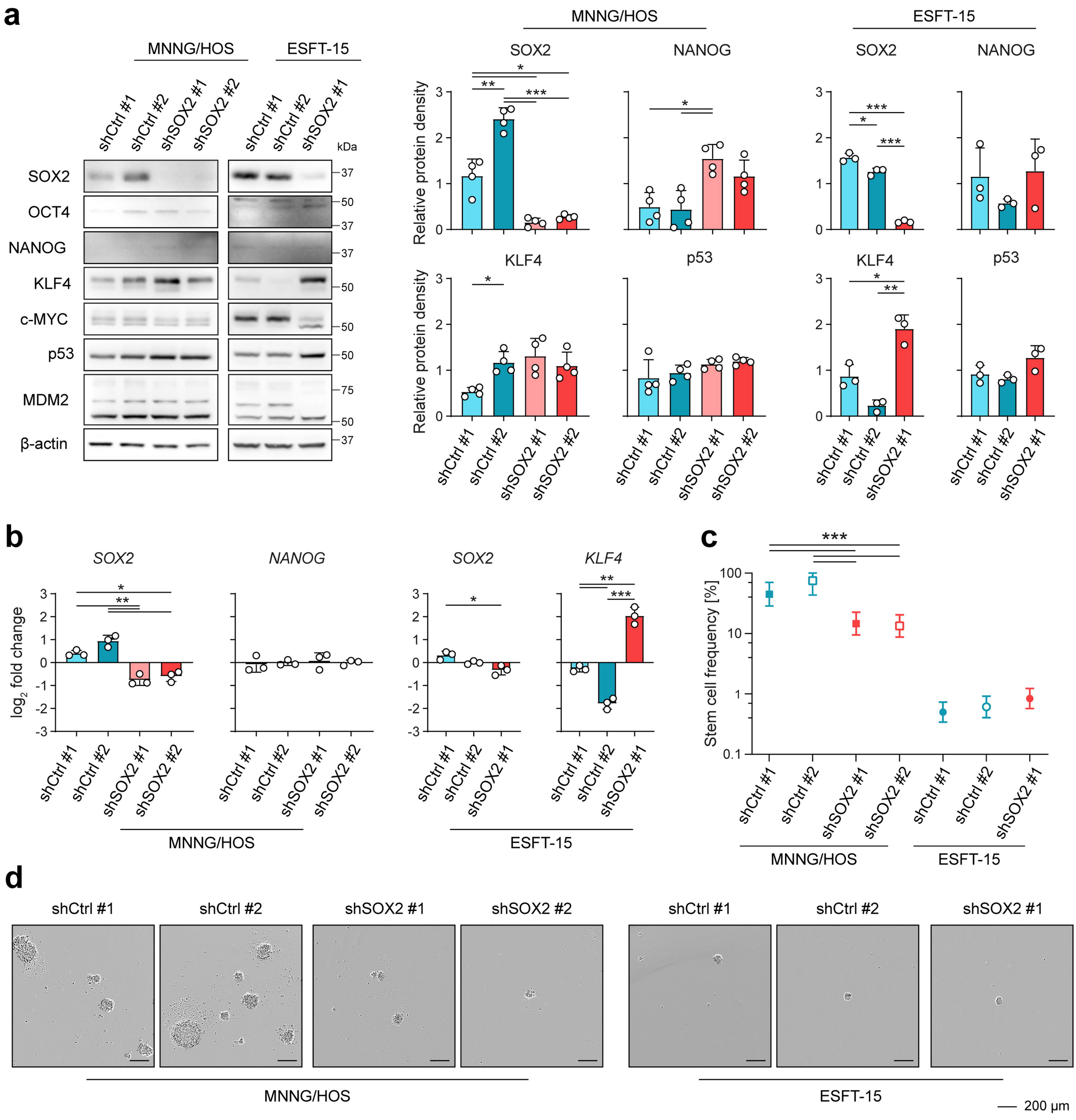
a
MNNG/HOS
ESFT-15
shCtrl #1
shCtrl #2
shSOX2 #1
shSOX2 #2
kDa
SOX2
OCT4
NANOG
KLF4
c-MYC
p53
MDM2
β-actin
37
50
75
Relative protein density
b
log2 fold change
c
Stem cell frequency [%]
d
200 µm

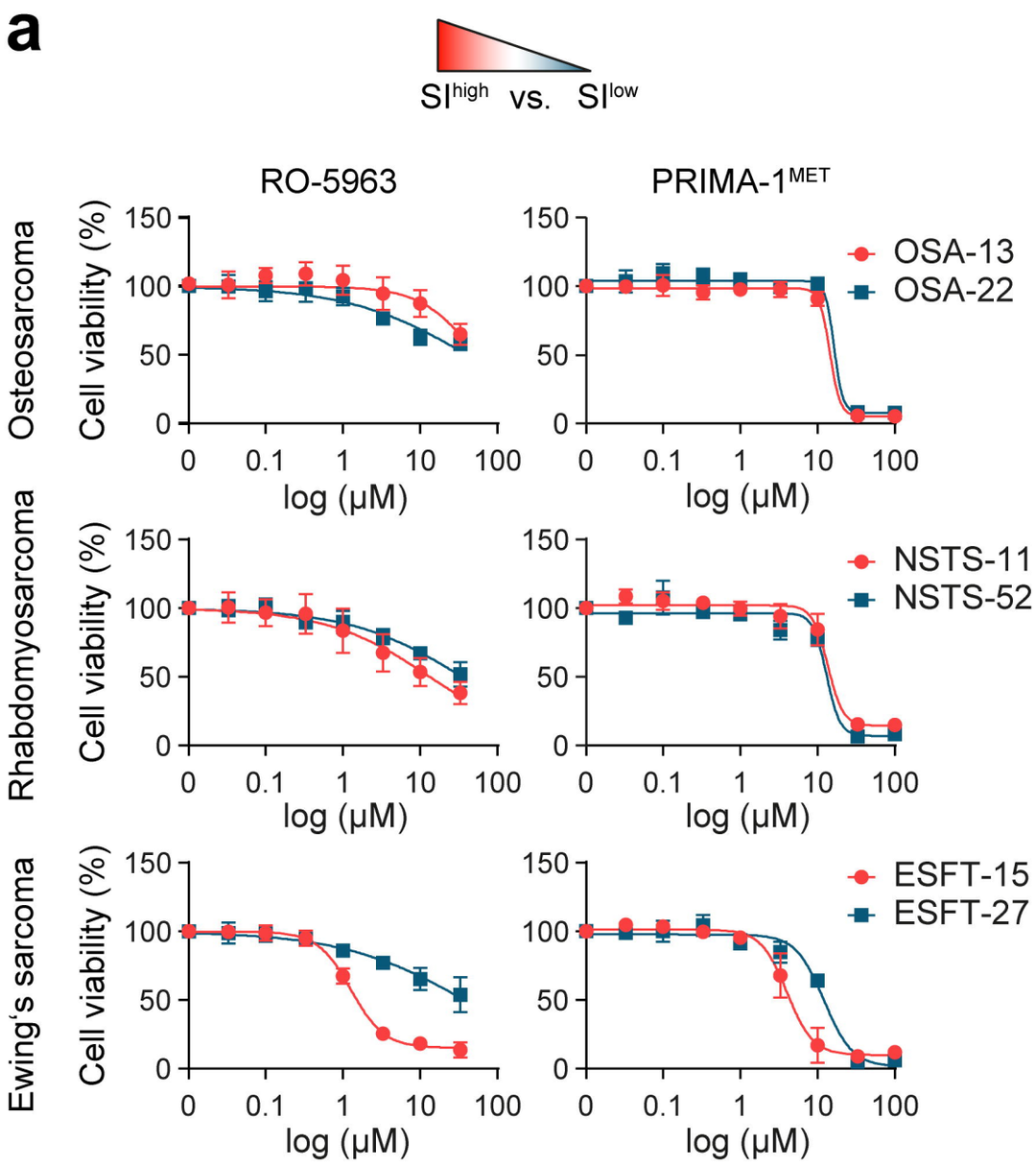
a
SI high vs. SI low
RO-5963
PRIMA-1MET
Osteosarcoma
Rhabdomyosarcoma
Ewing's sarcoma
Cell viability (%)
log (μM)
OSA-13
OSA-22
NSTS-11
NSTS-52
ESFT-15
ESFT-27

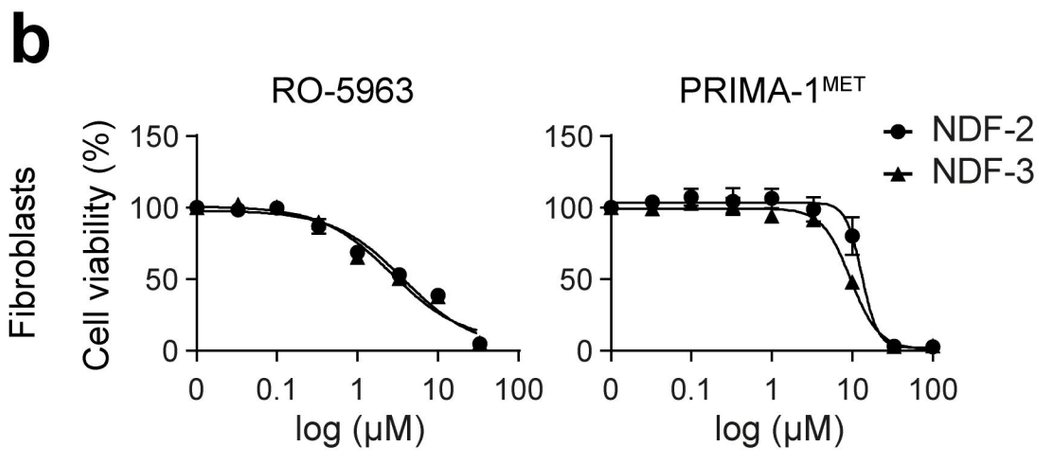
b
RO-5963
PRIMA-1MET
Fibroblasts
Cell viability (%)
log (μM)
NDF-2
NDF-3

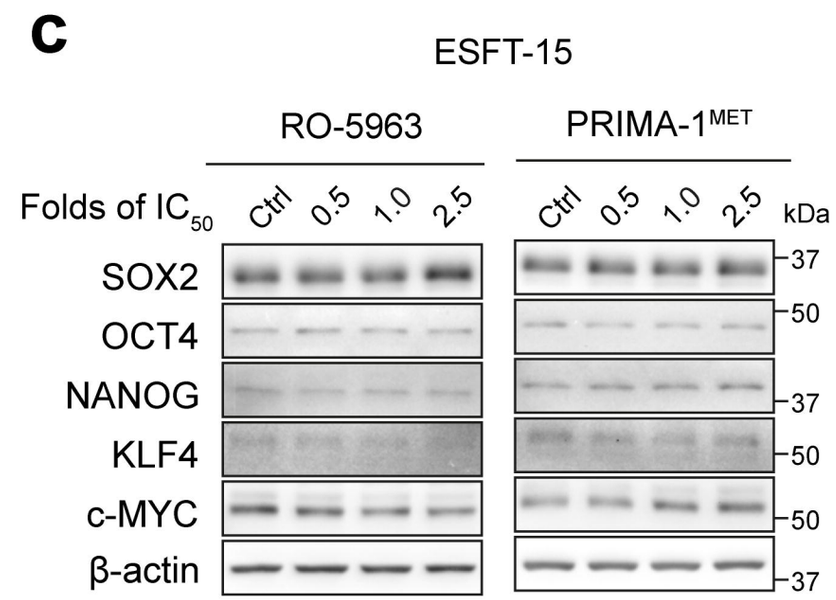
c
ESFT-15
RO-5963
PRIMA-1MET
Folds of IC50
Ctrl
0.5
1.0
2.5
kDa
SOX2
OCT4
NANOG
KLF4
c-MYC
β-actin
37
50

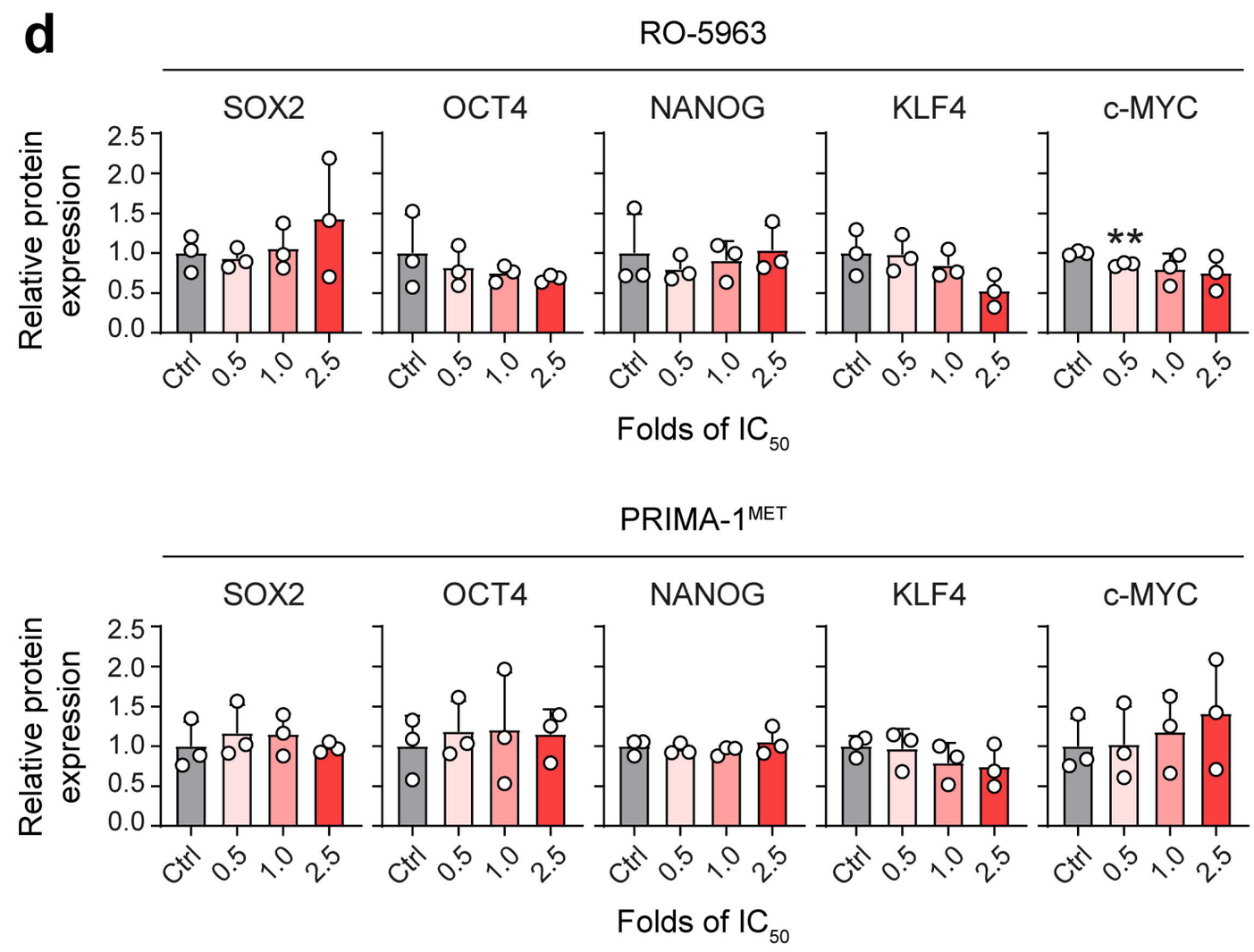
d
RO-5963
PRIMA-1MET
SOX2
OCT4
NANOG
KLF4
c-MYC
Relative protein expression
Folds of IC50
Ctrl
0.5
1.0
2.5
**

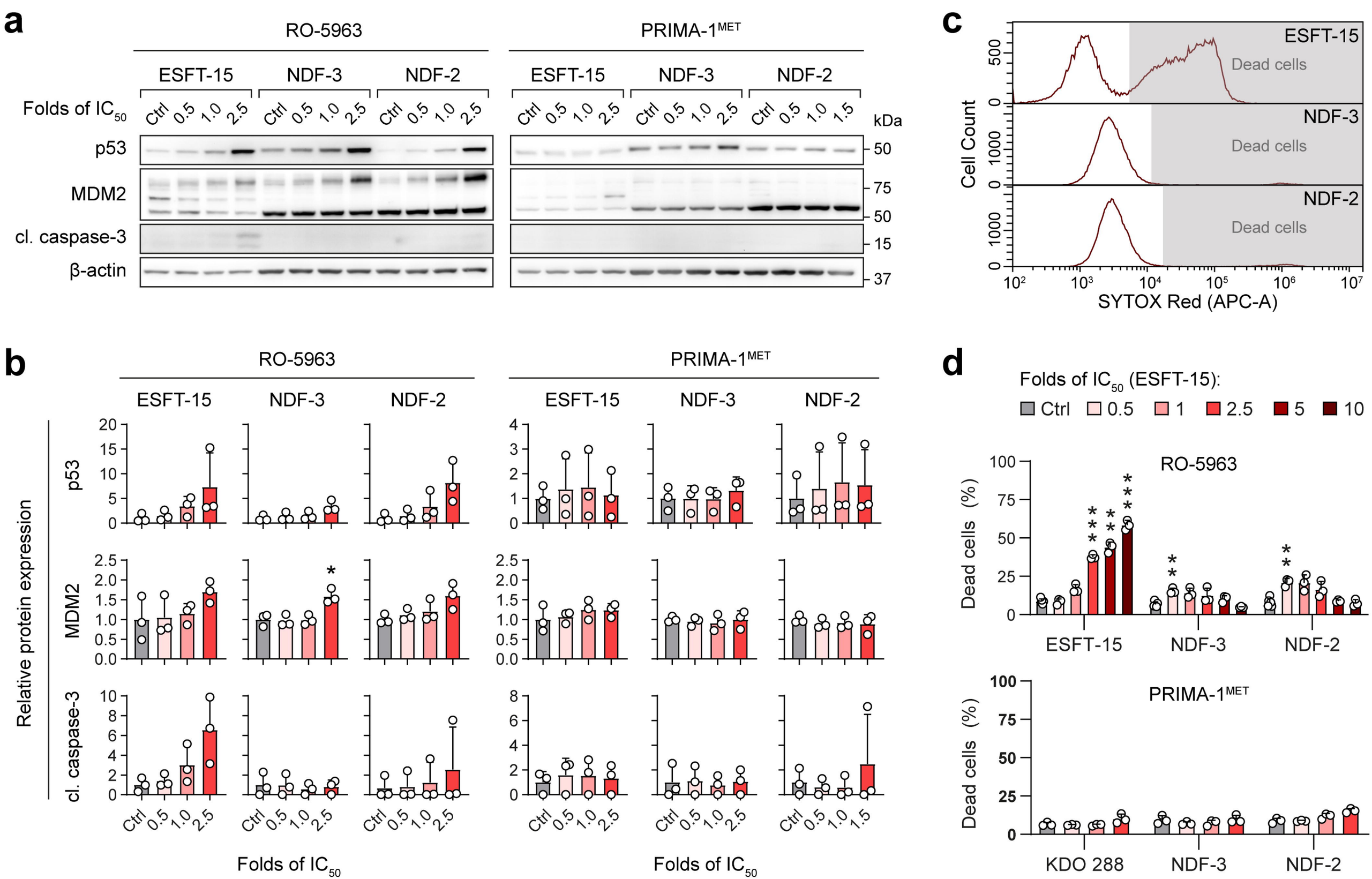
a
RO-5963
PRIMA-1MET
ESFT-15
NDF-3
NDF-2
Folds of IC50
Ctrl
0.5
1.0
2.5
1.5
kDa
p53
MDM2
cl. caspase-3
β-actin
50
75
50
15
37
b
Relative protein expression
Folds of IC50
c
Cell Count
Dead cells
SYTOX Red (APC-A)
d
Folds of IC50 (ESFT-15):
Ctrl
0.5
1
2.5
5
10
Dead cells (%)
KDO 288

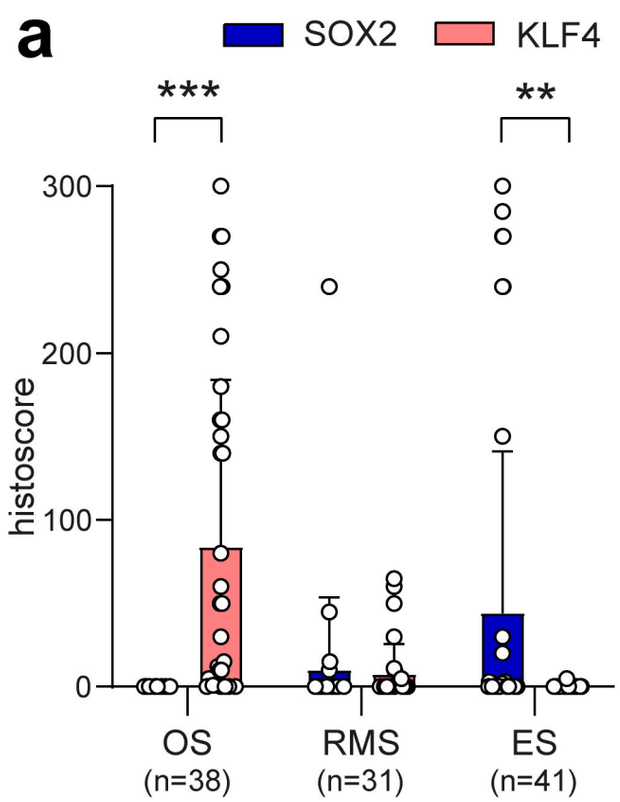
a
SOX2
KLF4
***
**
histoscore
300
200
100
0
OS
(n=38)
RMS
(n=31)
ES
(n=41)

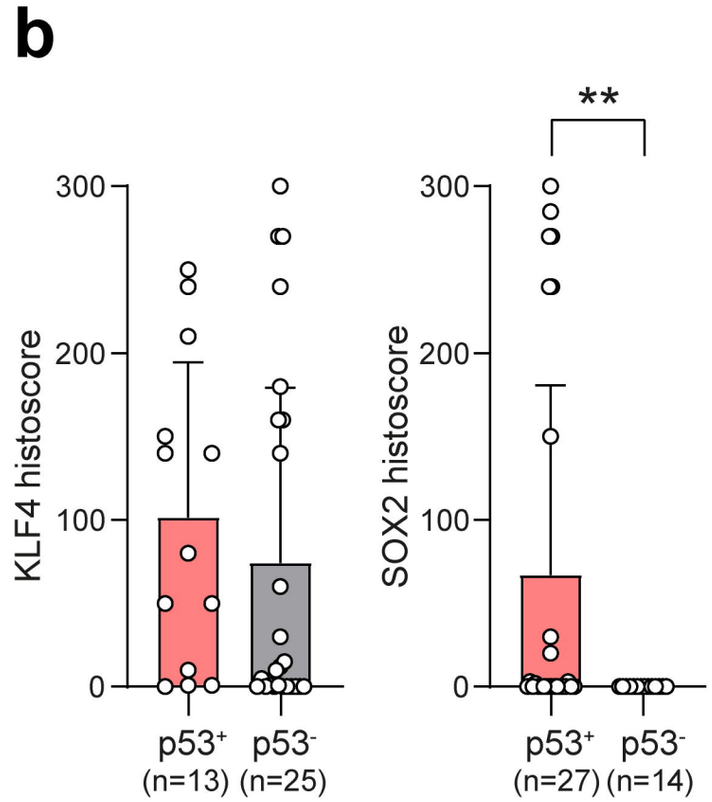
b
**
KLF4 histoscore
SOX2 histoscore
300
200
100
0
p53+
(n=13)
p53-
(n=25)
p53+
(n=27)
p53-
(n=14)

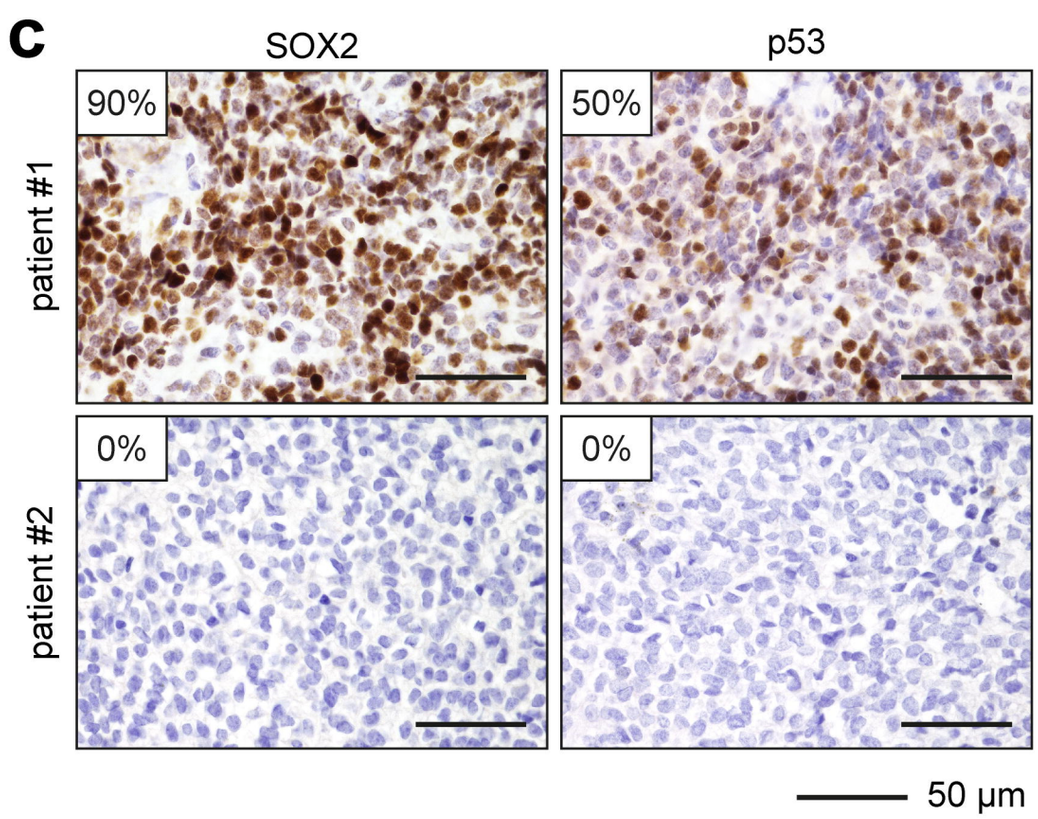
c
SOX2
p53
patient #1
patient #2
90%
50%
0%
0%
50 µm

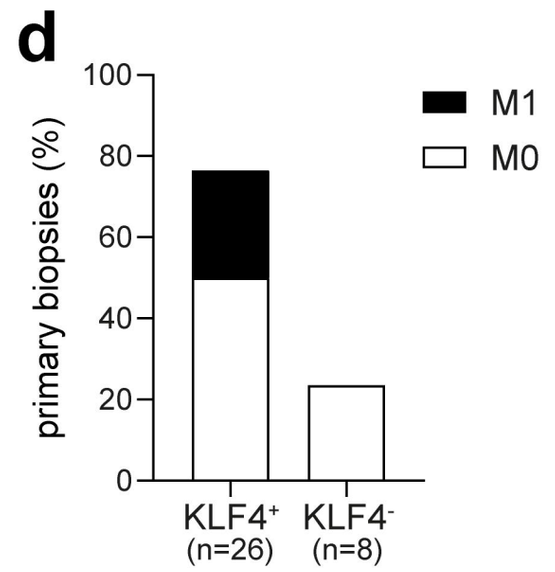
d
M1
M0
primary biopsies (%)
100
80
60
40
20
0
KLF4+
(n=26)
KLF4-
(n=8)

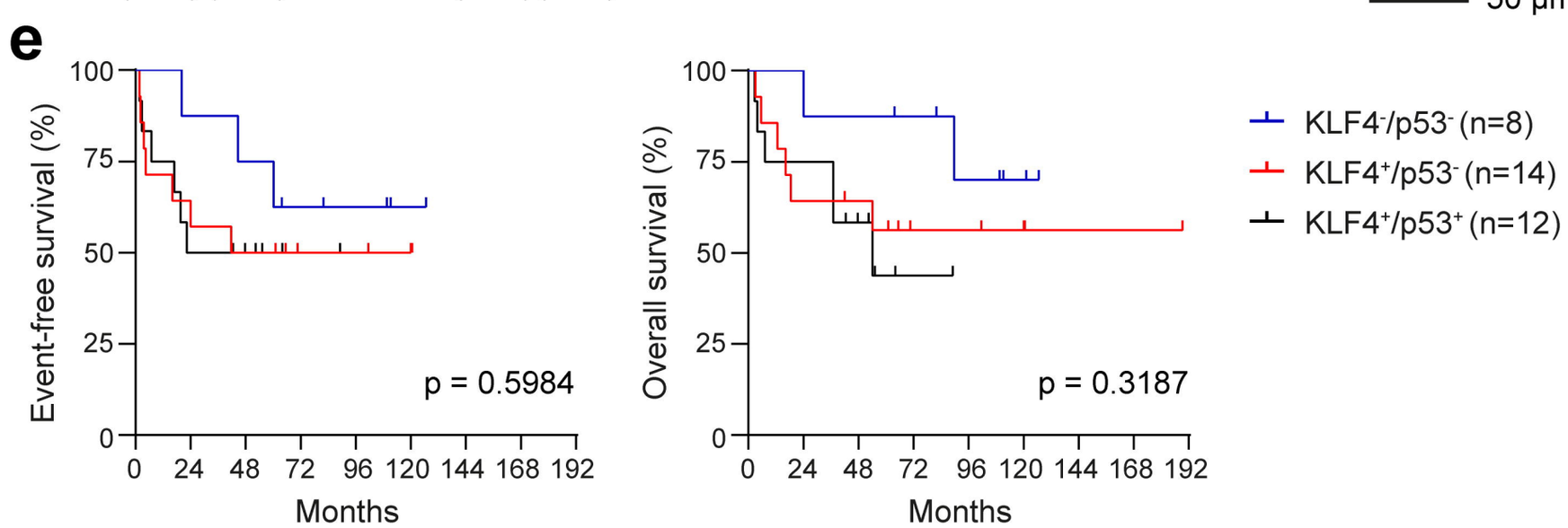
e
Event-free survival (%)
Overall survival (%)
100
75
50
25
0
0 24 48 72 96 120 144 168 192
Months
p = 0.5984
p = 0.3187
KLF4-/p53- (n=8)
KLF4+/p53- (n=14)
KLF4+/p53+ (n=12)

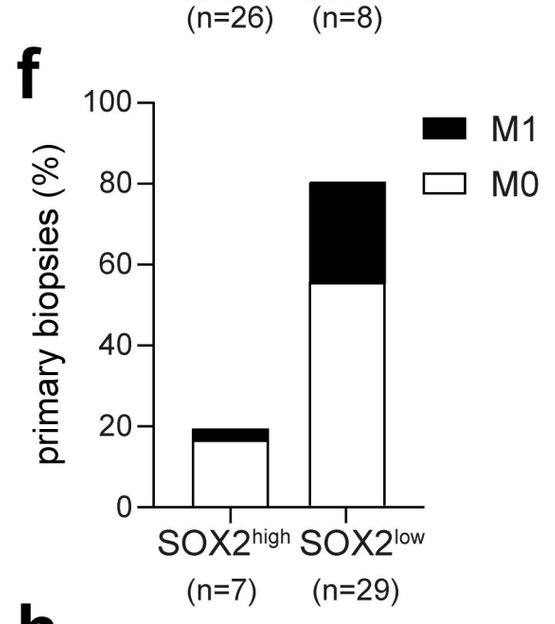
f
M1
M0
primary biopsies (%)
100
80
60
40
20
0
SOX2high
(n=7)
SOX2low
(n=29)

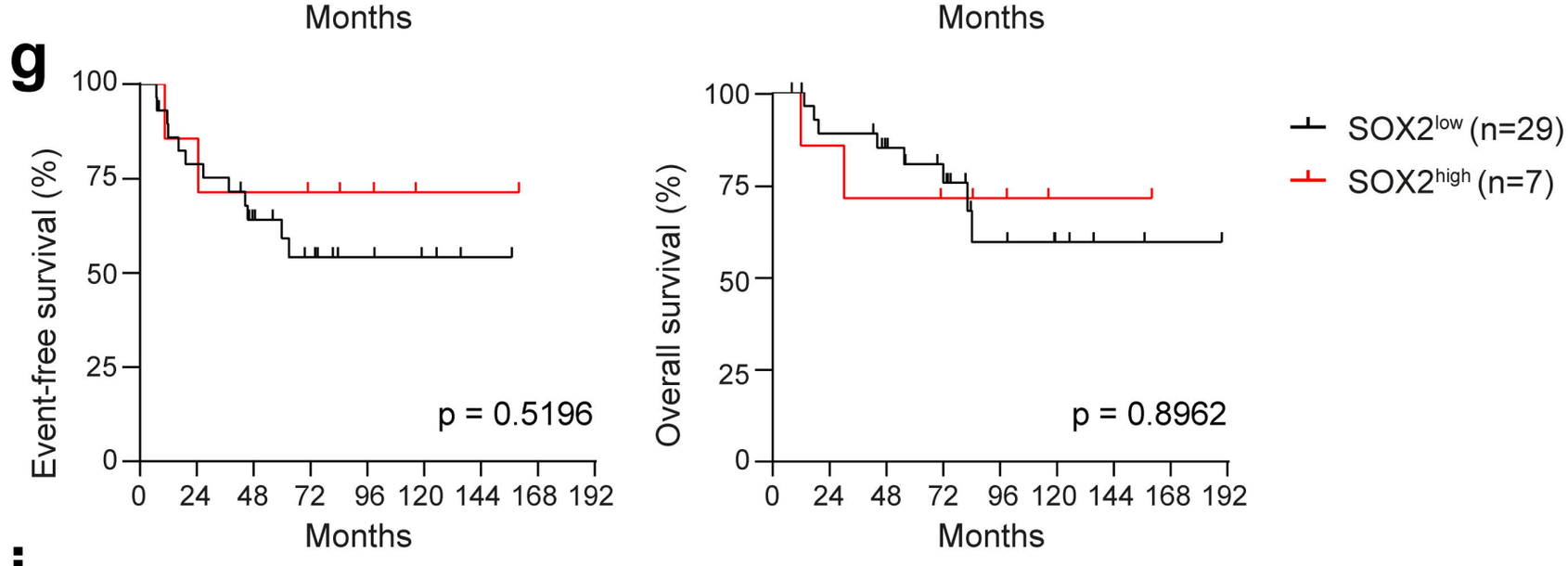
g
Event-free survival (%)
Overall survival (%)
100
75
50
25
0
0 24 48 72 96 120 144 168 192
Months
p = 0.5196
p = 0.8962
SOX2low (n=29)
SOX2high (n=7)

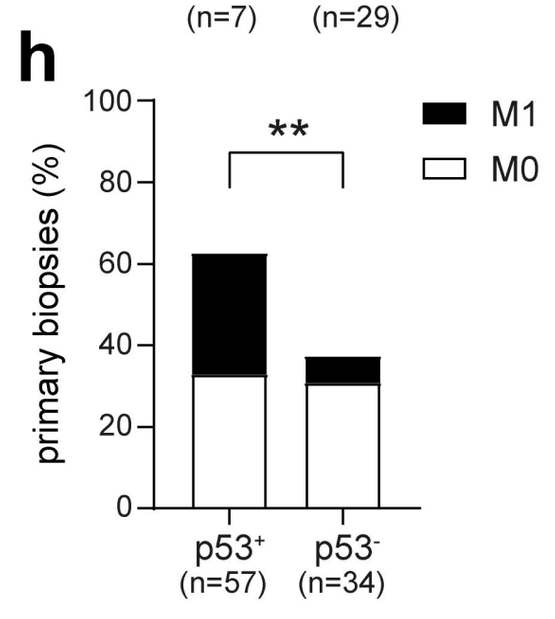
h
**
M1
M0
primary biopsies (%)
100
80
60
40
20
0
p53+
(n=57)
p53-
(n=34)

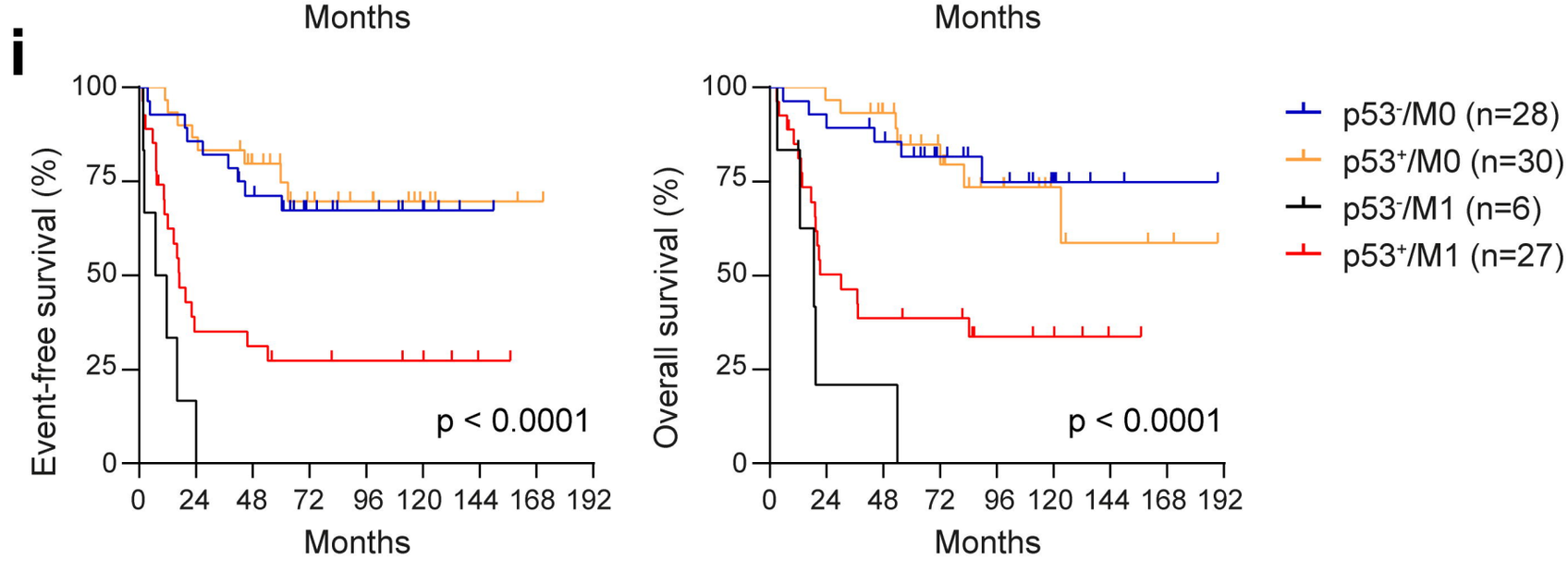
i
Event-free survival (%)
Overall survival (%)
100
75
50
25
0
0 24 48 72 96 120 144 168 192
Months
p < 0.0001
p < 0.0001
p53-/M0 (n=28)
p53+/M0 (n=30)
p53-/M1 (n=6)
p53+/M1 (n=27)